



## CO<sub>2</sub>, CH<sub>4</sub> and N<sub>2</sub>O fluxes along an altitudinal gradient in the northern Ecuadorean Andes: N<sub>2</sub>O consumption at higher altitudes

Paula Alejandra Lamprea Pineda<sup>1</sup>, Marijn Bauters<sup>1, 2</sup>, Hans Verbeeck<sup>2</sup>, Selene Baez<sup>3</sup>, Matti Barthel<sup>4</sup> and Pascal Boeckx<sup>1</sup>

5 <sup>1</sup>Isotope Bioscience Laboratory – ISOFYS, Department of Green Chemistry and Technology, Ghent University, Gent, 9000 Belgium

<sup>2</sup>Computational and Applied Vegetation Ecology – CAVELab, Department of Environment, Ghent University, Gent, 9000 Belgium

10 <sup>3</sup>Departamento de Biología, Escuela Politécnica Nacional del Ecuador, Ladrón de Guevara E11-253 y Andalucía, Quito, Ecuador

<sup>4</sup>Department of Environmental Systems Science, ETH Zurich, Zurich, 8092, Switzerland

Correspondence to: Paula Lamprea ([paulaalejandra.lampreapineda@ugent.be](mailto:paulaalejandra.lampreapineda@ugent.be))

Co-authors: [marijn.bauters@UGent.be](mailto:marijn.bauters@UGent.be), [hans.verbeeck@UGent.be](mailto:hans.verbeeck@UGent.be), [selene.baez@epn.edu.ec](mailto:selene.baez@epn.edu.ec), [matti.barthel@usys.ethz.ch](mailto:matti.barthel@usys.ethz.ch), [pascal.boeckx@UGent.be](mailto:pascal.boeckx@UGent.be)

15 Keywords: Tropical Forests - Soil CO<sub>2</sub>, CH<sub>4</sub> and N<sub>2</sub>O fluxes - Altitudinal Gradients - Source-partitioning N<sub>2</sub>O - Stable Isotopes.

### Abstract

Tropical forest soils are an important contributor to the global greenhouse (GHG) budget and understanding this ecosystem function is of vital importance for future global change and climate research. In this study, we quantified soil fluxes of carbon dioxide (CO<sub>2</sub>), methane (CH<sub>4</sub>) and nitrous oxide (N<sub>2</sub>O) of four tropical forest sites located along an altitudinal gradient from  
20 400 to 3010 m a.s.l. on the western flanks of the Andes in northern Ecuador. We assessed the physicochemical soil properties influencing these fluxes during the dry season, as well as the bulk isotopic signature of N<sub>2</sub>O. The CO<sub>2</sub> fluxes ranged between 55.3±12.1 and 137.6±32.8 mg C m<sup>-2</sup> h<sup>-1</sup>, with the highest and lowest emissions at the highest strata, at 3010 and 2200 m a.s.l., respectively. CH<sub>4</sub> fluxes at all sites exhibited a net consumption of atmospheric CH<sub>4</sub> and ranged between -74.4±25.0 μg C m<sup>-2</sup> h<sup>-1</sup> at 2200 m a.s.l. to -46.7±14.7 μg C m<sup>-2</sup> h<sup>-1</sup> at 3010 m a.s.l. Net fluxes of N<sub>2</sub>O ranged between -5.1±1.9 and 13.2±31.3 μg  
25 N m<sup>-2</sup> h<sup>-1</sup>, with a marked net sink at 2200 and 3010 m a.s.l., whereas a net source at 400 m. pH<sub>water</sub> and nitrate (NO<sub>3</sub><sup>-</sup>) content at 5 cm depth were able to explain 83% of the observed temporal (daily measurements) and spatial (four forest sites) variability of the CO<sub>2</sub> fluxes; indicating that an increase in pH<sub>water</sub> and NO<sub>3</sub><sup>-</sup> contents lead to an increase in CO<sub>2</sub> emissions. For CH<sub>4</sub> fluxes, it was not possible to obtain a statistically significant model to identify the physicochemical soil drivers responsible for the CH<sub>4</sub> consumption. For N<sub>2</sub>O, bulk density and pH<sub>water</sub> at 5 cm depth were negatively correlated to the N<sub>2</sub>O fluxes, but able to  
30 explain only 36% of the temporal and spatial variability. In addition, the bulk isotope N<sub>2</sub>O data confirmed that N<sub>2</sub>O reduction was at the basis of the observed net soil sink at higher altitudes. Finally, the soil GHG budget showed that all studied soils were net sources of GHG's. CO<sub>2</sub> emissions represented the largest component of the total soil GHG budget, CH<sub>4</sub> consumption was quite consistent along the elevation gradient, whereas N<sub>2</sub>O was highly variable, and the transition from sources to net



sinks at higher altitudes represented the biggest change in the net GHG balance. Overall, for non-CO<sub>2</sub> GHGs, we noticed a transition from a net source to a net GHG sink along altitude.

## 1 Introduction

In 2014, the Intergovernmental Panel on Climate Change (IPCC) released its Fifth Assessment Report (AR5) indicating that the atmospheric concentrations of the three major biogeochemical greenhouse gases (GHGs) (carbon dioxide - CO<sub>2</sub>, methane - CH<sub>4</sub> and nitrous oxide - N<sub>2</sub>O) have reached unprecedented levels. As such, current atmospheric concentrations indicate that in 2018, CO<sub>2</sub> (407.8±0.1 ppm), CH<sub>4</sub> (1869±2 ppb) and N<sub>2</sub>O (331.1±0.1 ppb) concentrations were 147%, 256% and 123%, higher compared to pre-industrial levels (before 1750) (WMO, 2019). A large proportion of CO<sub>2</sub> emissions are sourced by human activities, particularly fossil fuel burning and land use change. Similarly, the increase in CH<sub>4</sub> emissions is mainly due to fossil fuel and agriculture (60%), as well as for N<sub>2</sub>O, of which food production is the largest contributor to the N<sub>2</sub>O increase (Syakila and Kroeze, 2011).

Soils in terrestrial ecosystems play a vital role in the global GHG budget. Tropical forest soils, in particular, represent a net sink of carbon (C) (Pan et al. 2011), but they coincidentally are the largest natural source of N<sub>2</sub>O, with an estimated contribution of 14-23% to the annual, global N<sub>2</sub>O budget (Werner et al., 2007). In general, soil CO<sub>2</sub>, CH<sub>4</sub> and N<sub>2</sub>O production or consumption depends on microbiological processes driven by a wide range of abiotic and biotic characteristics. The combination of these processes ultimately determines if a soil is a net source or sink of GHGs. Under aerobic conditions, CO<sub>2</sub> is emitted to the atmosphere by autotrophic and heterotrophic respiration of vegetation and fauna (Dalal and Allen, 2008), while CH<sub>4</sub> is consumed by methanotrophic bacteria (Jang et al., 2006); although forest soils prone to inundation (anaerobic) emit CH<sub>4</sub> by methanogenic microorganisms (*Archaea* domain). On the other hand, N<sub>2</sub>O is emitted through denitrification or a number of alternative pathways (e.g. nitrification, nitrifier-denitrification, chemodenitrification, etc.; (Butterbach-Bahl et al., 2013; van Cleemput, 1998; Clough et al., 2017)). Overall, tropical forests emit on average 12.1 t CO<sub>2</sub>-C ha<sup>-1</sup>y<sup>-1</sup> (heterotrophic and autotrophic respiration), slightly smaller than the Net Primary Productivity (NPP) (12.5 t CO<sub>2</sub>-C ha<sup>-1</sup>y<sup>-1</sup>) i.e. the net C sink of tropical forests is ~ 0.4 t CO<sub>2</sub>-C ha<sup>-1</sup>y<sup>-1</sup>. In aerobic conditions, CH<sub>4</sub> fluxes vary from -1 to -40 kg CH<sub>4</sub> ha<sup>-1</sup>y<sup>-1</sup>, with an average consumption of -4 kg CH<sub>4</sub> ha<sup>-1</sup>y<sup>-1</sup>, while the mean rate of N<sub>2</sub>O emissions from tropical forest soils is 4.76±0.81 kg N<sub>2</sub>O ha<sup>-1</sup>y<sup>-1</sup> (Dalal and Allen, 2008), i.e. 2-3 times higher than the mean N<sub>2</sub>O emissions from temperate forest soils (1.57±0.56 kg N<sub>2</sub>O ha<sup>-1</sup>y<sup>-1</sup>; Chapui-Lardy et al., 2007; Van Groenigen et al., 2015). Despite de lower concentrations compared to CO<sub>2</sub> and CH<sub>4</sub>, N<sub>2</sub>O emissions have received increasing attention over the last decades because 1) the global warming potential of N<sub>2</sub>O is almost 300 times that of CO<sub>2</sub>, (IPCC, 2014b; Myhre et al., 2013), 2) N<sub>2</sub>O emissions contribute to the depletion of the stratospheric ozone layer (Portmann et al., 2012), and 3) they remain in the atmosphere for approximately 130 years (Myhre et al., 2013).

65



The understanding of the mechanisms and processes underlying GHG flux variability has greatly improved during the last decades (Butterbach-Bahl et al., 2013; Heil et al., 2016; Müller et al., 2015; Sousa Neto et al., 2011; Su et al., 2019; Teh et al., 2014). However, there is still (1) considerable uncertainty about the overall balances of many ecosystems (Castaldi et al., 2013; Heil et al., 2014; Kim et al., 2016; Pan et al., 2011; Purbopuspito et al., 2006), (2) a strong imbalance in field observations, 70 skewed to the Northern Hemisphere (Jones et al., 2016; Montzka et al., 2011), and (3) a bias towards quantification of emissions in lowland forests within the tropics (Müller et al., 2015; Purbopuspito et al., 2006). For instance, based on a compilation made of CO<sub>2</sub>, CH<sub>4</sub> and N<sub>2</sub>O fluxes in South America (Table S.3), there are only two studies on emissions in upper montane forests, while they represent 11% of the world's tropical forests (Müller et al., 2015; Teh et al., 2014). To further improve our understanding of tropical forest ecosystems on the global GHG balance, environmental gradients (elevational, 75 latitudinal, etc.) can offer great opportunities to study the influence of abiotic factors on biogeochemical processes under field conditions (Bauters et al., 2017a; Jobbágy and Jackson, 2000; Kahmen et al., 2011; Laughlin and Abella, 2007), which complements the knowledge on short term responses from experimental approaches. In the case of elevational gradients, these responses are driven by abiotic variables that co-vary with elevation, which, amongst others, creates a distinctly strong climate gradient over a short spatial distance (Bubb et al., 2004; Killeen et al., 2007; Körner, 2007; Myers et al., 2000).

80

Here, we present a study of the soil-atmosphere exchange of CO<sub>2</sub>, CH<sub>4</sub> and N<sub>2</sub>O along an altitudinal gradient in a Neotropical montane forest located on the western flanks of the Andes in northern Ecuador. We aimed (1) to determine the magnitude of the soil-atmosphere exchange of CO<sub>2</sub>, CH<sub>4</sub> and N<sub>2</sub>O during the dry season, and (2) to assess the main climatic and soil parameters that control these fluxes. By working along this altitudinal gradient, we wanted to explore the potential effect of 85 temperature - and other factors that co-vary with altitude - on the GHG budget of the forest soils. We expected the CO<sub>2</sub> fluxes to decrease with altitude, with higher emissions at lower altitudes in view of more ideal conditions (i.e. temperature and soil moisture); CH<sub>4</sub> fluxes to represent net sinks that increase (i.e. negative fluxes) with altitude, and mainly explained by soil moisture; and a decrease in N<sub>2</sub>O fluxes along the altitudinal gradient, with soil moisture and nitrogen (N) content as the main explanatory variables.

## 90 2 Materials and methods

### 2.1 Study areas

The field work was carried out along an altitudinal gradient from lowland (400 m a.s.l.) to upper montane evergreen forests (3010 m a.s.l.; Table 1) (FAO, 2017; Ministerio del Ambiente, 2015). We selected areas of well-preserved natural forests located on the western flanks of the Andes in northern Ecuador; specifically, in the Sierra region of the provinces of Imbabura 95 and Pichincha. Four study sites (Fig. S1) were selected: Río Silanche at 400 m a.s.l. (hereinafter: S\_400), Milpe at 1100 m a.s.l. (hereinafter: M\_1100), El Cedral at 2200 m a.s.l. (hereinafter: C\_2200) and Peribuela at 3010 m a.s.l. (hereinafter: P\_3010). Observations were made within one plot of about 20x20 m, established at each study site.



All sites experience two rainy seasons (March - April and October - November), with a mean annual precipitation (MAP) that varies on average between 900 and 3600 mm, and an adiabatic lapse rate of approx. 5 °C per 1000 m of altitude (Table 1) (Varela and Ron, 2018).

## 2.2 Sampling strategy

At all study areas, the sampling campaign took place from August 6<sup>th</sup> to September 28<sup>th</sup>, 2018, corresponding to the end of the dry season. One plot was selected for each site, and within each plot, five polyvinyl chloride (PVC) collars were installed to allow *in-situ* measurements using a static flux chamber method. The collars were inserted at random locations within the plots but guaranteeing at least 7 m distance between each one. The insertion of the collars was performed at least 12 h before the first measurements by applying even pressure across all points to minimize effects caused by soil disturbance. The chambers consisted of a PVC pipe hermetically sealed on top with a rubber-sealed lid. The chamber area was 0.0191 m<sup>2</sup> and the internal volume ranged between 3.63 and 3.98 L. Each chamber was equipped with sampling ports mounted with three-way valves, and a vent tube was installed to reduce pressure interferences.

Gas samples were collected mid-morning and measurement cycles on each site consisted of four consecutive gas measurements once per day for one hour and during five contiguous days. The samples were taken mid-morning to avoid extreme temperatures and we consider them as representative of a whole day (Collier et al., 2014; Luo and Zhou, 2006d). For these measurements, the collars were left in place for the duration of each measurement cycle; thus, the analysis per stratum lasted 1 week (i.e. 1 month for all measurements in the 4 strata). However, in order to assess a both short-term and long-term variation mainly related to weather conditions, the gas measurements were done first in August and consequently repeated in the next month (September).

Adjacent to each chamber (~ 1 m), one pit was dug for soil sampling, and intact soil cores were collected using stainless steel cylinders (diameter: 5.08 cm, height: 5.11 cm). The samples were taken at 5 and 20 cm depth once during the first month (August) of measurements. Each soil core was immediately packed into airtight zip-lock bags and once the sampling campaign was over, they were sent to Belgium for physicochemical soil analysis. Bulk density ( $\rho_b$ ) was measured by oven drying (75°C for 48 h) and weighing the soil samples. Soil porosity was derived from Eq. (1), assuming a particle density of 2.65 g cm<sup>-3</sup>. pH was measured by a potentiometric method using a pH-sensitive glass electrode, a standard reference electrode (HI 4222; Hanna Instrument, Bedfordshire, UK), and a volumetric ratio soil:liquid of 1:5 for pH<sub>water</sub> (distilled water) and pH<sub>KCl</sub> (1M KCl). NO<sub>3</sub><sup>-</sup> and NH<sub>4</sub><sup>+</sup> content was determined colorimetrically (Auto Analyzer 3; Bran and Luebbe, Norderstedt, Germany) after extractions performed with 1M KCl at room temperature and neutral pH. C and N concentrations (%C, %N), along with the stable N isotope signatures ( $\delta^{15}\text{N}$ ) of the soil samples, were determined at natural abundance by a Continuous Flow Element Analyzer (Automated Nitrogen Carbon Analyzer), interfaced with an Isotope-Ratio Mass Spectrometer (Sercon 20-20; Sercon,



Cheshire, UK). Moreover, the soil samples taken at 5 and 20 cm depth were combined to produce one composite sample associated to each site, and by means of the method described by the International Organization for Standardization (ISO 11277:2009), soil texture was determined. The classification was made according to the classification system of the United States Department of Agriculture (USDA, 2017); and the soil class was determined based on the classification of FAO and  
135 UNESCO: World Reference Base for Soil Resources (WRB) (FAO, 2007).

$$Porosity [\%] = \left(1 - \frac{\rho_b [g\ cm^{-3}]}{2.65 [g\ cm^{-3}]}\right) \cdot 100\% \quad (1)$$

Daily measurements of soil moisture, expressed as water-filled pore space (WFPS), were taken per site at 5 and 20 cm depth  
140 using soil moisture sensors (EC-5, Meter Environment, Pullman, Washington, USA) and data loggers (ProCheck, Meter Environment, Pullman, Washington, USA). Finally, soil temperature was determined daily for each measurement cycle and per chamber, by means of a thermometer inserted at 5 cm depth and approximately 10 cm from each chamber.

### 2.2.1 Soil-atmosphere exchange

12 h after the installation of the collars, the chambers were closed for a period of 1 h, and samples of 20 mL were taken with  
145 disposable syringes from the headspace air of the chambers every 20 minutes:  $T_1 = 0$ ,  $T_2 = 20$ ,  $T_3 = 40$  and  $T_4 = 60$  min;  $T_1$  or time-zero indicates the sample taken immediately after the chamber was closed. Moreover, prior to each sample collection, the syringe was flushed twice with air of the chamber to mix the chamber headspace and to avoid any possible stratification of them.

150 The 20 mL samples were injected in pre-evacuated 12 mL exetainer vials (over-pressurized), and once the sampling campaign was over, the samples were sent to Belgium for analysis by gas chromatography at Ghent University. For  $CH_4$  and  $CO_2$  analysis a gas chromatograph (Finnigan Trace GC Ultra; Thermo Electron Corporation, Milan, Italy) equipped with a flame ionization detector (FID) and a thermal conductivity detector (TCD) was used, respectively. For  $N_2O$ , another gas chromatograph equipped with an electron capture detector (ECD) (Shimadzu GC-14B; Shimadzu Corporation, Tokyo, Japan) was used.

### 155 2.2.2 $N_2O$ bulk isotopic composition

Two extra gas samples were taken for stable isotope analysis at the start ( $T_1$ ) and at the end ( $T_4$ ) of a chamber closure. These samples were taken only once per site and in only one of the chambers. For this, in addition to the small exetainer vials, pre-evacuated big serum vials (110 mL) were used to inject gas samples of 180 mL (over-pressured). At the end of the field campaign, the samples were transported to Switzerland (ETH Zurich) and analyzed for bulk  $^{15}N$  measurement of  $N_2O$  ( $\delta$   
160  $^{15}N^{Bulk}$ ) using a gas preparation unit (Trace Gas, Elementar, Manchester, UK) coupled to an Isotope Ratio Mass Spectrometer (IRMS) (IsoPrime100, Elementar, Manchester, UK). For measurement and calibration details see Verhoeven et al. (2019).



### 2.3 Data analysis

All statistical analyses were conducted in R Studio, version 3.5.2 (The R Core Team, 2019), and the statistical significance was reported at 95% confidence level ( $P \leq 0.05$ ), unless otherwise stated.

165

Mean values with standard deviations (SD) per site and depth were calculated for the physicochemical soil properties. The fluxes for each gas (CO<sub>2</sub>, CH<sub>4</sub> and N<sub>2</sub>O) were calculated by means of linear regressions using the four consecutive measurements of each measurement cycle. The slope of the regressions represented the flux. Thus, following the ideal gas law, and considering the head space volume of the chamber and the chamber area, the net gas flux was calculated by Eq. (2) (Collier et al., 2014; Dalal et al., 2008; Kutzbach et al., 2007):

170

$$F_c = \left( \frac{\Delta c [ppm]}{t [min]} \right) \cdot \left( \frac{P [atm]}{R [L atm mol^{-1} K^{-1}] \cdot T [K]} \right) \cdot (MW [g mol^{-1}]) \cdot \left( \frac{V_{ch} [L]}{A_{ch} [m^2]} \right) \quad (2)$$

where  $F_c$  corresponds to the net gas flux (CO<sub>2</sub>, CH<sub>4</sub> or N<sub>2</sub>O),  $\Delta c/t$  is the rate of change of the gas concentration within the chamber or the slope of the regression line [ppm min<sup>-1</sup> or  $\mu L L^{-1} min^{-1}$ ],  $P/RT$  corresponds to the ideal gas law used to convert concentration from volumetric to mass at normal temperature and pressure:  $P$  = absolute pressure (1 atm),  $R$  = gas law constant (0.08206 L atm mol<sup>-1</sup> k<sup>-1</sup>), and  $T$  = temperature (293 K);  $MW$  is the molecular weight of the gas (CO<sub>2</sub>-C: 12.01 g mol<sup>-1</sup>, N<sub>2</sub>O-N: 14.01 g mol<sup>-1</sup>),  $V_{ch}$  is the headspace volume of the chamber, and  $A_{ch}$  the area of the chamber. The goodness-of-fit was evaluated for every linear regression using the adjusted coefficient of determination ( $R^2$ ), and time series (concentration vs time) with  $R^2 < 0.60$  were excluded from further analysis.

175

180

For the purpose of evaluating if there were any statistical differences at each site between the fluxes obtained in August and September, a one-way ANOVA was performed per site; verifying for each case the respective assumptions (i.e. equality of variances and normality). Moreover, a linear model was fitted using the sites as a factorial explanatory variable per gas flux measurement to assess differences across sites, to estimate the effect sizes of the net fluxes, and to determine to which extent the variability of the net fluxes could be explained by these explanatories. For this, the validity of the model was evaluated through verification of assumptions of linearity, homoscedasticity (or equality of variances), and normality of the error terms; and due to the nature of the data in the measurements of N<sub>2</sub>O, the N<sub>2</sub>O fluxes were log-transformed to homogenize variances.

185

In order to determine the physicochemical soil characteristics able to explain to the greatest extent the net fluxes of CO<sub>2</sub>, CH<sub>4</sub> and N<sub>2</sub>O (response variable), a preliminary stepwise multiple linear regression was done for each soil gas. However, due to the low amount of data points (number of plots per altitude) and the small variability within plots, we averaged the measurements out, rather than to explicitly use separate measurements in a more complex linear mixed effect model. Therefore, we started with a full model that included all variables measured at 5 cm depth (predictors), and the average per plot and per

190



195 day of the fluxes measured only during the first month (August) (the soil samples for physicochemical soil properties were only taken in August). Then, using the “step” function of the “stats” package in R (The R Core Team, 2019) and the Akaike Information Criterion (AIC), a model was selected for each gas. Subsequently, the variance inflation factor (VIF) was calculated to avoid multicollinearity problems between predictors, and by means of the “vif” function from the “car” package in R (The R Core Team, 2019), along with a VIF threshold of  $< 3$ , the predictors with a higher VIF were excluded one by one.  
200 Finally, a simple linear regression was carried out for each flux with the retained predictors, verifying in each case the validity of the model and the respective assumptions (i.e. linearity, homoscedasticity and normality of the error terms).

The soil isotopic signature of  $N_2O$  was calculated using a two-source mixing model. Based on the conservation of mass depicted in Eq. (3) - where the atmospheric concentration of  $N_2O$  ( $C_a$ ) reflects the background atmospheric concentration of  
205 the gas ( $C_b$ ), plus the amount added by the source(s) ( $C_s$ ) - and including the isotope ratios of each component (4), the soil isotopic signature of  $N_2O$  - or  $\delta^{15}N_s^{Bulk}$  - can be calculated by Eq. (5). However, due to the nature of the data (very low  $N_2O$  concentrations), a minimum concentration difference of 20 ppb was defined as threshold to remove super low fluxes and thus, avoid larger uncertainties in the source calculation.

$$210 \quad C_a = C_b + C_s \quad (3)$$

$$\delta^{15}N_a^{Bulk} \cdot C_a = \delta^{15}N_b^{Bulk} \cdot C_b + \delta^{15}N_s^{Bulk} \cdot C_s \quad (4)$$

$$\delta^{15}N_s^{Bulk} = \frac{\delta^{15}N_a^{Bulk} \cdot C_a - \delta^{15}N_b^{Bulk} \cdot C_b}{C_a - C_b} \quad (5)$$

Finally, in order to compare the fluxes of the three GHGs measured (i.e.  $CO_2$ ,  $CH_4$  and  $N_2O$ ) and to determine the overall budget of the soils, the  $CO_2$ -eq emissions for each gas were calculated by means of Eq. (6), and by using a global warming  
215 potential (GWP) of 1, 28 and 265 for  $CO_2$ ,  $CH_4$  and  $N_2O$ , respectively (IPCC, 2014a). Moreover, the total GHG budget at each site was obtained by summing the  $CO_2$ -eq emissions of each gas (Myhre et al., 2013).

$$CO_2 - eq_i [mg \ m^{-2}h^{-1}] = flux_i [mg_i \ m^{-2}h^{-1}] \cdot GWP_i \quad (6)$$

where  $i$  refers to  $CO_2$ ,  $CH_4$  or  $N_2O$ .

## 220 3 Results

### 3.1 Physicochemical soil properties

Soils are Andosols and the soil texture was classified (USDA) between loam and sandy loam at all sites (WRB; Table 2). All sites had a relatively acidic soil;  $pH_{water}$  ranged from strong to medium acidic (4.61 - 5.69), with an increase in acidity with depth, except at P\_3010 (Table 2). The most acidic soil was found at S\_400 at 5 cm, although not significantly different from  
225 M\_1100 and C\_2200; whereas the least acidic one at P\_3010 at 5 cm depth, and only significantly different from M\_1100.



Except for P\_3010, NO<sub>3</sub>-N concentrations were 2-4 times higher at 5 cm compared to 20 cm depth; the highest variability was observed at S\_400, and in comparison to the other sites, P\_3010 seems to be depleted in NO<sub>3</sub>-N at both depths (0.8 – 3.6 μg g<sup>-1</sup>). In contrast, the highest concentration of NH<sub>4</sub>-N was obtained at P\_3010 at 20 cm, followed by S\_400 at 5 cm. However, at all sites, NH<sub>4</sub>-N concentrations at 5 cm were not significantly different from each other. Such as NO<sub>3</sub>-N, NH<sub>4</sub>-N also  
230 decreased with depth, except at P\_3010 where the increase at 20 cm with respect to 5 cm was almost doubling. Higher N contents were measured at 5 cm compared to 20 cm depth at all sites; and S\_400 exhibited the highest content at both depths, 1.3-1.4 times higher than any other N percentage at the same depth, and even 4 times higher than any other N percentage at 20 cm depth. The C content showed a general decrease with depth at all sites, with the highest percentage at S\_400 at 5 cm, and the lowest one at M\_1100 at 20 cm. Higher δ<sup>15</sup>N signatures were obtained at 20 cm compared to 5 cm depth; at S\_400 the soil  
235 was most enriched in <sup>15</sup>N, and P\_3010 showed the most depleted one.

Soil temperature decreased with altitude with a gradient of -4.2 °C per 1000 m, with no statistical difference between months. WFPS increased significantly with depth at all sites during both months (Fig. S2), except at C\_2200 in September. The lowest WFPS at 5 cm depth was obtained at C\_2200 (16.8%±2.5) and P\_3010 (14.4%±0.3) in August and September, respectively,  
240 whereas the highest one at M\_1100 at 20 cm in both months (August: 75.9%±0.3; September: 71.9%±6.3).

### 3.2 Greenhouse gas fluxes

In general, all sites were sources of CO<sub>2</sub> (Fig. 1a, Table 3). Except for P\_3010, mean CO<sub>2</sub> emissions were higher in September compared to August, but due to the high variability in the measurements, there was no significant difference between months at M\_1100 and P\_3010 ( $P > 0.05$ ). The lowest and highest emissions were observed at C\_2200 and P\_3010, respectively, in  
245 both months, and all sites were significant predictors and able to explain 56% of the variability of CO<sub>2</sub> emissions during the field campaign (Fig. 1a).

All mean CH<sub>4</sub> fluxes were negative, indicating a net flux from the atmosphere to the soil (Fig. 1b, Table 3). Although the mean CH<sub>4</sub> fluxes (except for P\_3010) were higher in September compared to August, there was no significant difference ( $P > 0.05$ )  
250 between months at any site. Moreover, the linear model performed for CH<sub>4</sub> only explained 3% of the variability.

Finally, the mean N<sub>2</sub>O fluxes showed a general negative trend with increasing altitude (Fig. 1c). A marked net N<sub>2</sub>O consumption was observed at the sites located at 2200 and 3010 m a.s.l., and besides these sites, M\_1100 also acted as a net sink in September; however, there was no significant difference ( $P > 0.05$ ) in any plot between months. The highest  
255 consumption was observed in August at P\_3010, while the highest emission was in September at M\_1100 (Table 3). On the other hand, the fitted linear model explained 65% of the variability of the N<sub>2</sub>O fluxes during the field campaign.



260 Although only monthly average fluxes will be discussed, the large variability observed with most of the gas fluxes (Table 3 and Fig. 1) are the result of the spatial (i.e. differences in GHG fluxes between chambers) and temporal (i.e. differences in GHG fluxes per day) variability within each site.

### 3.3 Linear regressions with physicochemical soil characteristics

265 Changes in  $\text{pH}_{\text{water}}$  and  $\text{NO}_3\text{-N}$  at 5 cm depth explained 83% of the temporal (daily measurements) and spatial (four sites) variability of  $\text{CO}_2$  fluxes in August (Table 4). Both predictors were positively correlated with  $\text{CO}_2$  emissions, thus,  $\text{pH}_{\text{water}}$  ( $P < 0.001$ ) and  $\text{NO}_3\text{-N}$  content ( $P = 0.51$ ) were positively related to  $\text{CO}_2$  fluxes. For  $\text{CH}_4$  consumption, it was not possible to obtain a model since none of the predictors were retained during the stepwise selection. In case of  $\text{N}_2\text{O}$  fluxes, bulk density ( $P = 0.07$ ) and  $\text{pH}_{\text{water}}$  ( $P = 0.06$ ) at 5 cm depth explained 36% of the temporal and spatial variability in August. Although both predictors were close to the threshold ( $P = 0.05$ ) and considered as non-significant, they indicate a negative correlation where every increase in bulk density and  $\text{pH}_{\text{water}}$  lead to a decrease in  $\text{N}_2\text{O}$  fluxes.

### 3.4 Isotopic signature of $\text{N}_2\text{O}$ ( $\delta^{15}\text{N}_s^{\text{Bulk}}$ )

270  $\delta^{15}\text{N}_s^{\text{Bulk}}$  ranged from -13.08 to 11.54‰, with the lowest and highest isotopic signature observed at S\_400 (September) (Fig. 2, Table S1). During both months,  $\delta^{15}\text{N}_s^{\text{Bulk}}$  values of M\_1100, C\_2200 and P\_3010 exhibited  $^{15}\text{N}$  enrichments, and all of them reflected chambers where negative fluxes were obtained i.e. consumption of  $\text{N}_2\text{O}$  from the atmosphere to the soil (Table S1).

### 3.5 Soil GHG Budget

275 The average soil GHG balance indicates that all plots during August and September are considered as sources of GHGs, largely driven by  $\text{CO}_2$  emissions (Fig. 3a), and with the highest compensation from  $\text{CH}_4$  consumption (Fig. 3b). During both months, the highest and lowest  $\text{CO}_2\text{-eq}$  emissions were obtained at P\_3010 (August: 499.6, September: 450.6  $\text{mg CO}_2\text{-eq m}^{-2}\text{h}^{-1}$ ) and at C\_2200 (August: 200.3, September: 248.3  $\text{mg CO}_2\text{-eq m}^{-2}\text{h}^{-1}$ ), respectively; in both cases,  $\text{N}_2\text{O}$  and  $\text{CH}_4$  consumption resulted in a ~1% offset of the total  $\text{CO}_2\text{-eq}$  emissions.

## 280 4 Discussion

### 4.1 GHG fluxes and correlations

#### 4.1.1 $\text{CO}_2$ fluxes

285 Across our study sites, P\_3010 exhibited the highest soil  $\text{CO}_2$  emissions (Fig. 1a and Table 3). Even though an increase in temperature (up to an optimum of ca. 50°C; Luo and Zhou, 2006a; Oertel et al., 2016), moisture-WFPS (up to an optimum 60%; Dalal and Allen, 2008; Luo and Zhou, 2006b) and  $\text{pH}_{\text{water}}$  (up to an optimum 7; Oertel et al., 2016) generally lead to higher emissions of  $\text{CO}_2$ , P\_3010 is the site with the lowest temperature and WFPS, but with the highest soil  $\text{pH}_{\text{water}}$ . Indeed,



under acid conditions, Sitaula et al. (1995) reported a 2 to 12 fold decrease in CO<sub>2</sub> emissions with decreasing pH<sub>water</sub> from 4.0 to 3.0; and Persson & Wiren (1989) indicated a decrease in CO<sub>2</sub> emissions of 83 and 78% with a decrease in pH<sub>water</sub> from 3.8 to 3.4 and 4.8 to 4.0, respectively. This is also supported by Luo & Zhou (2006a), Oertel et al. (2016), Reth et al., (2005) and Wang et al., (2010) who have reported positive correlations between soil pH<sub>water</sub> and CO<sub>2</sub> fluxes. Hence, this dominant role of pH<sub>water</sub> in the overall CO<sub>2</sub> budget is also apparent across our study range. Nonetheless, shifts in C allocation could also give rise to shifts in CO<sub>2</sub> emissions, and thus support the increase observed in the site located at the highest altitude (P\_3010). As such, an increase in fine root biomass is expected in tropical mountain forests compared to lowland forests. In fact, a study carried out in the South Ecuadorian Andes from 1050 to 3060 m a.s.l., indicates a positive linear correlation ( $R^2 = 0.87$ ,  $P = 0.01$ ) between fine root biomass and altitude, arguing that imbalances or limitations in resource (water and/or nutrients) availability at higher altitudes may be the cause (Leuschner et al., 2007). Consequently, the observed increase in CO<sub>2</sub> emissions at high altitude might be further driven by an increase in root biomass as the latter has been shown to be positively correlated with soil respiration (Han et al., 2007; Luo and Zhou, 2006a; Reth et al., 2005; Silver et al., 2005).

In contrast to P\_3010, the low emissions observed at C\_2200 could be attributed to (1) the lower WFPS, (2) the lower contents of C and N, and (3) the higher bulk density. Indeed, the lowest content of water was observed at this site in August at 5 cm depth, and exactly in this month, the lowest emissions of CO<sub>2</sub> were obtained. The low contents of C and N exhibited in C\_2200 (indeed, the lowest from all the sites), could have hampered the CO<sub>2</sub> emissions, since an increase in C content normally leads to higher levels of respiration, and N itself is required for plants and soil microorganisms to grow (Dalal and Allen, 2008; Luo and Zhou, 2006a; Oertel et al., 2016). In additions, this site also had the highest soil bulk density (i.e. lowest porosity), which could have led to a decrease in soil respiration either by a physical impediment for root growth or by a decrease in soil aeration for microbial activities (Dilustro et al., 2005; Luo and Zhou, 2006c, 2006a). For instance, Kowalenko et al. (1978) reported an almost double CO<sub>2</sub> emission from a clayey loamy soil (7.04 mg CO<sub>2</sub>-C m<sup>-2</sup> h<sup>-1</sup>) than from a sandy soil (3.75 mg CO<sub>2</sub>-C m<sup>-2</sup> h<sup>-1</sup>), and Dilustro et al. (Dilustro et al., 2005) reported an overall 1.5 increase in CO<sub>2</sub> emissions from a clayey soil (171.07 mg CO<sub>2</sub>-C m<sup>-2</sup> h<sup>-1</sup>) with respect to a sandy one (117.07 mg CO<sub>2</sub>-C m<sup>-2</sup> h<sup>-1</sup>).

Finally, our measurements are enveloped by earlier work when framed in a broader and pantropical context (Table S3, Fig. 4). However, although a quantitative comparison is difficult to make due to differences in e.g. sampling durations (single seasons, whole year cycles or only specific dates), sampling frequencies (sub-daily, daily or monthly), measuring methods, intrinsic site properties, etc., our fluxes are well below most of the CO<sub>2</sub> fluxes reported for South America, except for a study performed in Brazil at 130 m a.s.l. (17.4 mg CO<sub>2</sub>-C m<sup>-2</sup> h<sup>-1</sup>) (Verchot et al., 2000). Moreover, although it is not common to obtain higher fluxes at higher altitudes, only one study performed in Peru, between 2811 – 2962 m a.s.l., showed a flux similar in magnitude (dry season: 120 mg CO<sub>2</sub>-C m<sup>-2</sup> h<sup>-1</sup>, wet season: 170 mg CO<sub>2</sub>-C m<sup>-2</sup> h<sup>-1</sup>) (Jones et al., 2016) to our flux obtained at P\_3010.



#### 4.1.2 CH<sub>4</sub> fluxes

320 In general, all sites acted as net sinks for CH<sub>4</sub> (i.e. uptake of atmospheric CH<sub>4</sub> by soils). During the whole field campaign only one chamber at one site (S\_400) and a specific date (08/09/2018) showed a net source of CH<sub>4</sub> (45.82 μg CH<sub>4</sub>-C m<sup>-2</sup> h<sup>-1</sup>). However, there were no statistical differences between months. The mean CH<sub>4</sub> fluxes were quite similar even between sites, and there was no significant linear regression with the physicochemical soil characteristics able to explain the CH<sub>4</sub> fluxes. All sites exhibited indeed a high temporal and spatial variability (Fig. 1b and Table 3), but WFPS was measured in only one  
325 chamber per site and generalized for the site itself. Moreover, due to the arrangement of the data for the linear regression (see section 2.3.), taking average-plot values instead of point-chamber values could have led to a loss of ‘explaining power’ in this case.

CH<sub>4</sub> consumption is generally higher compared to the majority of CH<sub>4</sub> fluxes reported in the literature (for tropical forest soils  
330 in South America (Table S.3, Fig. 5). Only the fluxes observed in Peru between 1532–1769 m a.s.l. (dry season: -45.82 μg CH<sub>4</sub>-C m<sup>-2</sup> h<sup>-1</sup>) and 2811–2962 m a.s.l. (dry season: -66.71 μg CH<sub>4</sub>-C m<sup>-2</sup> h<sup>-1</sup>) (Jones et al., 2016) are of the same order of magnitude as our fluxes; keeping in mind that we measured at the end of the dry season. However, as mentioned previously for CO<sub>2</sub> emissions, this comparison must be treated with caution since there are different variables influencing the final results. Even so, except for one study carried out in Ecuador at 400 m a.s.l. (19.37 μg CH<sub>4</sub>-C m<sup>-2</sup> h<sup>-1</sup>), all fluxes depicted in Fig. 5 and  
335 measured during a dry season (DS), represent a sink of CH<sub>4</sub>, which is supported by the fact that humid tropical forests are responsible of 10% to 20% of the global soil sink for atmospheric CH<sub>4</sub> (Verchot et al., 2000).

#### 4.1.3 N<sub>2</sub>O fluxes

Only S\_400 (both months) and M\_1100 (September) (i.e. plots located at the lower locations) acted as net sources of N<sub>2</sub>O (Fig. 1c, Table 3). In contrast, the lowest flux was observed in the plot located at the highest stratum (P\_3010) during August  
340 and September, which showed a general net consumption. The high emissions obtained at the lowest strata corroborate with literature data on lowland tropical forests (Butterbach-Bahl et al., 2004, 2013; Koehler et al., 2009) and are mainly attributed to (1) soil water content, (2) temperature, and (3) N availability.

Firstly, N<sub>2</sub>O emissions in tropical forest soils are predominantly governed by WFPS, which influences microbial activity, soil  
345 aeration and thus diffusion of N<sub>2</sub>O out of the soil (Davidson et al., 2006; Werner et al., 2007). Ideally, the highest emissions via denitrification are observed between 60–80% WFPS, but they can vary between 50–80% or 60–90% depending on the soil physical properties (Butterbach-Bahl et al., 2013; Dalal and Allen, 2008; Davidson et al., 2006; Oertel et al., 2016). At lower percentages (optimum: 20%), nitrification takes place and although N<sub>2</sub>O can be produced as well, it yields a higher potential for NO production (Davidson et al., 2006; Oertel et al., 2016). As a second main driver for N<sub>2</sub>O emissions, and in comparison  
350 to CO<sub>2</sub> emissions, denitrification is very sensitive to rising temperatures (Oertel et al., 2016). An increase in temperature leads



to an increase in soil respiration and thus to a depletion of O<sub>2</sub> concentrations, which is indeed a major driver in N<sub>2</sub>O emissions. Moreover, rising temperatures lead to a positive feedback in microbial metabolism; the stimulation of mineralization and nitrification processes induces an increase in the availability of substrates for denitrification, and thus to an increase in N<sub>2</sub>O emissions (Butterbach-Bahl et al., 2013; Sousa Neto et al., 2011). Hence, the high emissions observed at S\_400 can also be supported by the high temperatures observed at this site; which are indeed the highest from all sites (Fig. S1). Finally, the dependency of N<sub>2</sub>O emissions on WFPS and temperature is affected by substrate availability (NO<sub>3</sub><sup>-</sup>) which was also the highest at S\_400 (almost 2.5 times higher than the second highest content observed). High contents of NO<sub>3</sub><sup>-</sup> give an indication of an open or “leaky” N cycle with higher rates of mineralization, nitrification and thus N<sub>2</sub>O emissions (Davidson et al., 2006). Moreover, NO<sub>3</sub><sup>-</sup> is normally preferred as an electron acceptor over N<sub>2</sub>O and it can also inhibit the rate of N<sub>2</sub>O consumption to N<sub>2</sub> (Dalal and Allen, 2008).

In contrast to the low elevation sites where net N<sub>2</sub>O emissions were observed, P\_3010 presented the highest consumption (negative values, i.e. fluxes from the atmosphere to the soil), followed by C\_2200. From 37 valid measurements only 1 resulted in net emission at P\_3010 (range: -12.91 to 1.33 μg N<sub>2</sub>O-N m<sup>-2</sup> h<sup>-1</sup>), whereas from 36 measurements, 20 resulted in net emissions at C\_2200 (range: -11.10 to -0.31 μg N<sub>2</sub>O-N m<sup>-2</sup> h<sup>-1</sup>). Net N<sub>2</sub>O consumption is often related to N-limited ecosystems. Indeed, at low NO<sub>3</sub><sup>-</sup> concentrations, atmospheric or gaseous N<sub>2</sub>O may be the only electron acceptor left for denitrification (Chapui-Lardy et al., 2007; Goossens et al., 2001). Studies performed by Teh et al. (Teh et al., 2014) and Müller et al. (Müller et al., 2015) in the Southern Peruvian and Ecuadorian Andes, respectively, related the decrease in N<sub>2</sub>O emissions - and thus the potential for N<sub>2</sub> production in soils - at high elevations to differences in NO<sub>3</sub><sup>-</sup> availability.

In this case, P\_3010 had the lowest content of NO<sub>3</sub><sup>-</sup>, along with the lowest soil δ<sup>15</sup>N, which clearly reflects the shift towards a more closed N cycle at higher elevations (Bauters et al., 2017b). Moreover, this was the site with 1) the highest content of clay and hence more microsites for N<sub>2</sub>O reduction, 2) the lowest soil water content (% of WFPS) and hence more diffusion of atmospheric N<sub>2</sub>O into the soil, 3) the highest pH-value, which could have alleviated inhibition of the nitrous oxide reductase at low pH, and 4) the highest CO<sub>2</sub> emissions observed, which could have indeed led to the development of anaerobic microsites where denitrification could have occurred (Chapui-Lardy et al., 2007). This is also valid for M\_1100, where N<sub>2</sub>O consumption was observed in August (3 out of 7 valid measurements; range: -10.48 to 9.18 μg N<sub>2</sub>O-N m<sup>-2</sup> h<sup>-1</sup>), whereas N<sub>2</sub>O emission in September (5 out of 16 valid measurements; range: -9.67 to 94.42 μg N<sub>2</sub>O-N m<sup>-2</sup> h<sup>-1</sup>). Although samples of soils were not taken in September, this month represents the transition or the beginning of the wet season in the region. Thus, it is expected to have an increase in available soil N due to the accumulation of litter during the dry season and the following but rapid mineralization after soil rewetting at the beginning of the rainy season, which could have indeed led to pulses of higher N<sub>2</sub>O emissions (Werner et al., 2007).



385 Contrary to CO<sub>2</sub> emissions, pH<sub>water</sub> negatively affected N<sub>2</sub>O emissions ( $R^2 = 0.36$ ). This relation has been already reported  
previously (Baggs et al., 2010; Chapui-Lardy et al., 2007; Wrage et al., 2001), and pH has been considered as a “master  
variable” to predict N transformations (Baggs et al., 2010). As a second predictor, bulk density also exhibited a negative  
correlation with N<sub>2</sub>O emissions. Reflecting the fact that higher values of bulk density are translated into less oxygen diffusion  
and thus, more anaerobic sites ideal for the reduction of N<sub>2</sub>O to N<sub>2</sub>. Likewise, Klefoth et al. (2014) observed a decrease in  
N<sub>2</sub>O fluxes of about ~ 71% when soil bulk density increased by only 0.13 units.

390

Finally, in comparison to other studies done in tropical forest soils in South America (Table S.3, Fig. 6), our N<sub>2</sub>O emissions  
(i.e. S\_400 in both months and M\_1100 in September) are in the same range as other fluxes reported in e.g. Ecuador (400  
m.a.s.l.: 7.53 and 7.36 μg N<sub>2</sub>O-N m<sup>-2</sup> h<sup>-1</sup>) and Brazil (400 m a.s.l.: 10 μg N<sub>2</sub>O-N m<sup>-2</sup> h<sup>-1</sup>; 1000 m.a.s.l.: 9.0 μg N<sub>2</sub>O-N m<sup>-2</sup> h<sup>-1</sup>)  
(Sousa Neto et al., 2011). The fluxes at the highest strata, however, seem to be relatively unique within a broader and  
395 pantropical context (Fig. 6). There are only two studies performed at comparable altitudes in South America; the first one in  
the Southern Ecuadorian Andes (2000 m a.s.l.: 2.05±0.64; and 3000 m a.s.l.: 0.47±0.62 μg N<sub>2</sub>O-N m<sup>-2</sup> h<sup>-1</sup>; Müller et al., 2015),  
and the second one in the Southern Peruvian Andes (1700 m a.s.l.: 40.83±9.58 (dry season), 6.67±5.24 (wet season); and 2700  
m a.s.l.: 7.92±7.08 (dry season), 0.83±9.17 (wet season); Teh et al., 2014). But, even though N<sub>2</sub>O consumption was observed  
in point measurements, all of them showed a net emission. From this, and based on previous observations, it seems that (1)  
400 N<sub>2</sub>O studies in the tropics are biased toward lowland forests (Müller et al., 2015; Purbopuspito et al., 2006), and (2) our results  
along with the low fluxes (and even negative data points) reported especially in the Andes, highlight the importance of a  
probably unaccounted sink of N<sub>2</sub>O at high altitudes; keeping in mind that tropical montane forests represent 11% of the world’s  
tropical forests (Müller et al., 2015).

#### 405 4.2 Isotopic signature of N<sub>2</sub>O ( $\delta^{15}N_s^{Bulk}$ )

Previous studies have indicated that during the reduction of N<sub>2</sub>O to N<sub>2</sub>, N<sub>2</sub>O-reductase fractionates against <sup>15</sup>N (Barford et al.,  
1999; Butterbach-Bahl et al., 2013; Menyailo and Hungate, 2006; Pérez et al., 2000). Consequently, complete denitrification  
i.e. consumption of N<sub>2</sub>O, leads to a <sup>15</sup>N enrichment of the residual N<sub>2</sub>O, and thus to higher  $\delta^{15}N_s^{Bulk}$  values (Park et al., 2011)  
relative to the atmospheric bulk N<sub>2</sub>O composition (6.3‰; (Harris et al., 2017)). This indeed is reflected in the enriched  $\delta^{15}N_s^{Bulk}$   
410 values measured during N<sub>2</sub>O consumption while the N<sub>2</sub>O bulk signature during N<sub>2</sub>O production was highly depleted compared  
to that of atmospheric N<sub>2</sub>O (two samples taken in September at S\_400) (Fig. 2; Table S1). This is also in line with Park et al.  
(2011) and Pérez et al. (2000) who have attributed  $\delta^{15}N_s^{Bulk}$  values between -22 and 2‰ in natural tropical forest soils to  
denitrification. Therefore, in addition to the soil isotope signatures, the bulk N<sub>2</sub>O isotope signatures confirm the net N<sub>2</sub>O  
consumption at higher altitudes, and net N<sub>2</sub>O emission at lower altitudes, and rule out that our net consumption rates are due  
415 to sampling artefacts.



### 4.3 Soil GHG Budget

The differences in fluxes for each GHG are clearly visualized in Fig. 3. The high CO<sub>2</sub> emissions observed at P\_3010 give rise to the highest CO<sub>2</sub>-eq emissions, and in terms of non-CO<sub>2</sub> GHG, this plot also exhibited the highest sink due to CH<sub>4</sub> and N<sub>2</sub>O consumption. However, it is important to mention that the calculated CO<sub>2</sub>-eq emissions for CO<sub>2</sub> reflect only the impact of soil emissions (heterotrophic and autotrophic respiration) on the soil GHG budget, excluding photosynthesis and aboveground respiration. Therefore, based on the fluxes here obtained, the upland soils from our study clearly show a marked sink of non-CO<sub>2</sub> GHG. Even so, besides this and the known potential for C sequestration in tropical forests, the marked CH<sub>4</sub> and N<sub>2</sub>O sinks observed in this case, enhances the importance and protection of tropical forests, not only in terms of biodiversity and ecosystem services, but also as means of mitigation options to curb global warming.

### 5 Conclusions

Overall, we found that our CO<sub>2</sub> fluxes are well below most of the CO<sub>2</sub> fluxes reported in literature for tropical forest soils, with an unusual but marked increase at the highest altitude, mainly explained by soil pH and root biomass. Moreover, our CH<sub>4</sub> uptake fluxes are among the highest in the tropics (i.e. highest consumption of atmospheric CH<sub>4</sub>) and reiterate the role of humid tropical forest soils as a known CH<sub>4</sub> sink. Contrary to the net N<sub>2</sub>O emissions observed in the lowest strata, the net consumption at higher elevation seems to be quite unique and reflects (1) the worldwide bias of N<sub>2</sub>O studies toward lowland forests, (2) the need of coupling environmental and physicochemical soil variables with microbial analyses, and (3) the importance of conserving upland forest for N<sub>2</sub>O consumption. This net N<sub>2</sub>O uptake was confirmed independently by soil and N<sub>2</sub>O <sup>15</sup>N isotope signatures. Finally, although an altitudinal gradient was selected to evaluate the potential effect of temperature - and other factors that co-vary with altitude - on the GHG budget of the forest soils, our results for CO<sub>2</sub>, CH<sub>4</sub> and N<sub>2</sub>O fluxes clearly reflect the “complex” interplay of different environmental controls and physicochemical soil characteristics rather than a generalized trend related to altitude.

### Supplementary information

**Fig. S1.** Overview map with the location of the study areas.

**Fig. S2.** Monthly average soil temperature (°C)±standard deviations (SD).

**Fig. S3.** Monthly average water-filled pore space (WFPS)±standard deviations (SD).

**Table S1.**  $\delta^{15}N_S^{Bulk}$  values and N<sub>2</sub>O fluxes.

**Table S.2.** Measured and estimated CO<sub>2</sub>, CH<sub>4</sub> and N<sub>2</sub>O fluxes from tropical forest soils of South America.

### Author contributions

M.Bauters, H.V., SB. and P.B. developed the project; P.L. and M. Bauters carried out the field work and analyzed the data. All authors contributed to the ideas presented and edited the manuscript.



### Competing interests

450 The authors declare that they have no conflict of interest.

### Acknowledgments

This research has been supported by Ghent University, the VLIR-UOS South Initiative COFOREC (EC2018SIN223A103). We also thank Mindo Cloud Forest Foundation, El Cedral Ecologde and the Escuela Politécnica Nacional del Ecuador, for the  
455 logistic support in Ecuador. M. Barthel was supported through ETH Zurich core funding provided to Johan Six.

### References

- Baggs, E. M., Smales, C. L. and Bateman, E. J.: Changing pH shifts the microbial source as well as the magnitude of N<sub>2</sub>O emission from soil, *Biol. Fertil. Soils*, 46, 793–805, doi:10.1007/s00374-010-0484-6, 2010.
- Barford, C. C., Montoya, J. P., Altabet, M. A. and Mitchell, R.: Steady-state nitrogen isotope effects of N<sub>2</sub> and N<sub>2</sub>O production  
460 in *Paracoccus denitrificans*, *Appl. Environ. Microbiol.*, 65(3), 989–994, doi:10.1128/aem.65.3.989-994.1999, 1999.
- Bauters, M., Verbeeck, H., Demol, M., Bruneel, S., Taveirne, C., Van Der Heyden, D., Cizungu, L. and Boeckx, P.: Parallel functional and stoichiometric trait shifts in South American and African forest communities with elevation, *Biogeosciences*, 14, 5313–5321, doi:10.5194/bg-14-5313-2017, 2017a.
- Bauters, M., Verbeeck, H., Demol, M., Bruneel, S., Taveirne, C., Van der Heyden, D., Cizungu, L. and Boeckx, P.: Parallel  
465 functional and stoichiometric trait shifts in South American and African forest communities with elevation, *Biogeosciences*, 14(April), 5313–5321, doi:10.5194/bg-2017-136, 2017b.
- Bubb, P., May, I., Miles, L. and Sayer, J.: *Cloud Forest Agenda*, in United Nations Environment Programme-World Conservation Monitoring Centre, p. 33, Cambridge, UK. [online] Available from: [http://www.unep-wcmc.org/index.html?http://www.unep-wcmc.org/resources/publications/UNEP\\_WCMC\\_bio\\_series/20.htm~main](http://www.unep-wcmc.org/index.html?http://www.unep-wcmc.org/resources/publications/UNEP_WCMC_bio_series/20.htm~main), 2004.
- 470 Butterbach-Bahl, K., Kock, M., Willibald, G., Hewett, B., Buhagiar, S., Papen, H. and Kiese, R.: Temporal variations of fluxes of NO, NO<sub>2</sub>, N<sub>2</sub>O, CO<sub>2</sub>, and CH<sub>4</sub> in a tropical rain forest ecosystem, *Global Biogeochem. Cycles*, 18, 1–11, doi:10.1029/2004GB002243, 2004.
- Butterbach-Bahl, K., Baggs, E. M., Dannenmann, M., Kiese, R. and Zechmeister-boltenstern, S.: Nitrous oxide emissions from soils: how well do we understand the processes and their controls?, *Phil Trans R Soc B*, 368, 1–20, doi:20130122, 2013.
- 475 Castaldi, S., Bertolini, T., Valente, a., Chiti, T. and Valentini, R.: Nitrous oxide emissions from soil of an African rain forest in Ghana, *Biogeosciences*, 10(6), 4179–4187, doi:10.5194/bg-10-4179-2013, 2013.
- Chapui-Lardy, L., Wrage, N., Metay, A., Chotte, J.-L. and Bernoux, M.: Soils, a sink for N<sub>2</sub>O? A review, *Glob. Chang. Biol.*, 13, 1–17, doi:10.1111/j.1365-2486.2006.01280.x, 2007.
- van Cleemput, O.: Subsoils: chemo-and biological denitrification, N<sub>2</sub>O and N<sub>2</sub> emissions, *Nutr. Cycl. Agroecosystems*, 52,



- 480 187–194, doi:10.1023/a:1009728125678, 1998.
- Clough, T. J., Lanigan, G. J., de Klein, C. A. M., Sainur Samar, M., Morales, S. E., Rex, D., Bakken, L. R., Johns, C., Condon, L. M., Grant, J. and Richards, K. G.: Influence of soil moisture on codenitrification fluxes from a urea-affected pasture soil, *Sci. Rep.*, 7, 1–12, doi:10.1038/s41598-017-02278-y, 2017.
- Collier, S. M., Ruark, M. D., Oates, L. G., Jokela, W. E. and Dell, C. J.: Measurement of greenhouse gas flux from agricultural  
485 soils using static chambers, *J. Vis. Exp.*, 90, 1–8, doi:10.3791/52110, 2014.
- Dalal, R. C. and Allen, D. E.: TURNER REVIEW No. 18 Greenhouse gas fluxes from natural ecosystems, *Aust. J. Bot.*, 56, 369–407, 2008.
- Dalal, R. C., Allen, D. E., Livesley, S. J. and Richards, G.: Magnitude and biophysical regulators of methane emission and consumption in the Australian agricultural, forest, and submerged landscapes: A review, *Plant Soil*, 309, 43–76,  
490 doi:10.1007/s11104-007-9446-7, 2008.
- Davidson, E. A., Yoko Ishida, F. and Nepstad, D. C.: Effects of an experimental drought on soil emissions of carbon dioxide, methane, nitrous oxide, and nitric oxide in a moist tropical forest, *Glob. Chang. Biol.*, 10, 718–730, doi:10.1111/j.1529-8817.2003.00762.x, 2004.
- Davidson, E. A., Keller, M., Erickson, H. E., Verchot, L. V. and Veldkamp, E.: Testing a conceptual model of soil emissions  
495 of nitrous and nitric oxides, *Bioscience*, 50, 667–680, doi:10.1641/0006-3568(2000)050[0667:tacmos]2.0.co;2, 2006.
- Dilustro, J. J., Collins, B., Duncan, L. and Crawford, C.: Moisture and soil texture effects on soil CO<sub>2</sub> efflux components in southeastern mixed pine forests, *For. Ecol. Manage.*, 204, 85–95, doi:10.1016/j.foreco.2004.09.001, 2005.
- FAO: Digital Soil Map of the World, GeoNetwork [online] Available from: <http://www.fao.org/geonetwork/srv/en/main.home?uuid=446ed430-8383-11db-b9b2-000d939bc5d8> (Accessed 1 May 2019),  
500 2007.
- FAO: National forest assessments - Country projects. Overview - Ecuador. Proyecto evaluación nacional forestal del Ecuador [National forestry evaluation project of Ecuador], [online] Available from: <http://www.fao.org/forestry/17847/en/ecu/> (Accessed 1 March 2019), 2017.
- Fick, S. E. and R.J. Hijmans: Worldclim 2: New 1-km spatial resolution climate surfaces for global land areas., *Int. J. Climatol.*,  
505 2017.
- Goossens, A., Visscher, A. De, Boeckx, P. and Cleemput, O. Van: Two-year field study on the emission of N<sub>2</sub>O from coarse and middle-textured Belgian soils with different land use, *Nutr. Cycl. Agroecosystems*, 60, 23–34, doi:10.1023/A:1012695731469, 2001.
- Van Groenigen, J. W., Huygens, D., Boeckx, P., Kuyper, T. W., Lubbers, I. M., Rütting, T. and Groffman, P. M.: The soil n cycle: New insights and key challenges, *Soil*, 1(1), 235–256, doi:10.5194/soil-1-235-2015, 2015.
- Han, G., Zhou, G., Xu, Z., Yang, Y., Liu, J. and Shi, K.: Biotic and abiotic factors controlling the spatial and temporal variation of soil respiration in an agricultural ecosystem, *Soil Biol. Biochem.*, 39, 418–425, doi:10.1016/j.soilbio.2006.08.009, 2007.
- Harris, E., Henne, S., Hüglin, C., Zellweger, C., Tuzson, B., Ibraim, E., Emmenegger, L. and Mohn, J.: Tracking nitrous oxide



- emission processes at a suburban site with semicontinuous, in situ measurements of isotopic composition, *J. Geophys. Res.*,  
515 122(3), 1850–1870, doi:10.1002/2016JD025906, 2017.
- Heil, J., Wolf, B., Brüggemann, N., Emmenegger, L., Tuzson, B., Vereecken, H. and Mohn, J.: Site-specific  $^{15}\text{N}$  isotopic signatures of abiotically produced  $\text{N}_2\text{O}$ , *Geochim. Cosmochim. Acta*, 139, 72–82, doi:10.1016/j.gca.2014.04.037, 2014.
- Heil, J., Vereecken, H. and Brüggemann, N.: A review of chemical reactions of nitrification intermediates and their role in nitrogen cycling and nitrogen trace gas formation in soil, *Eur. J. Soil Sci.*, 67, 23–39, doi:10.1111/ejss.12306, 2016.
- 520 IPCC: Annex II: Glossary. *Climate Change 2014: Synthesis Report. Contribution of Working Groups I, II and III to the Fifth Assessment Report of the Intergovernmental Panel on Climate Change*, Geneva, Switzerland., 2014a.
- IPCC: AR5 synthesis report. *Climate Change 2014: Synthesis report. Contribution of working groups I, II, and III to the fifth assessment report of the Intergovernmental Panel on Climate Change*, Geneva, Switzerland., 2014b.
- Jang, I., Lee, S., Hong, J. H. and Kang, H.: Methane oxidation rates in forest soils and their controlling variables: A review  
525 and a case study in Korea, *Ecol. Res.*, 21, 849–854, doi:10.1007/s11284-006-0041-9, 2006.
- Jobbágy, E. G. and Jackson, R. B.: The vertical distribution of soil organic carbon and its relation to climate and vegetation, *Ecol. Appl.*, 10(2), 423, doi:10.2307/2641104, 2000.
- Jones, S. P., Diem, T., Huaraca Quispe, L. P., Cahuana, A. J., Reay, D. S., Meir, P. and Teh, Y. A.: Drivers of atmospheric methane uptake by montane forest soils in the southern Peruvian Andes, *Biogeosciences*, 13, 4151–4165, doi:10.5194/bg-13-  
530 4151-2016, 2016.
- Kahmen, A., Sachse, D., Arndt, S. K., Tu, K. P., Farrington, H., Vitousek, P. M. and Dawson, T. E.: Cellulose  $\delta^{18}\text{O}$  is an index of leaf-to-air vapor pressure difference (VPD) in tropical plants, *PNAS*, 108(5), 1981–1986, doi:10.1073/pnas.1018906108, 2011.
- Keller, M., Kaplan, W. A. and Wofsy, S. C.: Emissions of  $\text{N}_2\text{O}$ ,  $\text{CH}_4$  and  $\text{CO}_2$  from tropical forest soils, *J. Geophys. Res.*,  
535 91, 11791–11802, doi:10.1029/jd091id11p11791, 1986.
- Killeen, T. J., Douglas, M., Consiglio, T., Jørgensen, P. M. and Mejia, J.: Dry spots and wet spots in the Andean hotspot, *J. Biogeogr.*, 34(8), 1357–1373, doi:10.1111/j.1365-2699.2006.01682.x, 2007.
- Kim, D. G., Thomas, A. D., Pelster, D., Rosenstock, T. S. and Sanz-Cobena, A.: Greenhouse gas emissions from natural ecosystems and agricultural lands in sub-Saharan Africa: Synthesis of available data and suggestions for further research,  
540 *Biogeosciences*, 13(16), 4789–4809, doi:10.5194/bg-13-4789-2016, 2016.
- Klefoth, R. R., Clough, T. J., Oenema, O. and Van Groenigen, J.-W.: Soil bulk density and moisture content influence relative gas diffusivity and the reduction of nitrogen-15 nitrous oxide, *Vadose Zo. J.*, 13, 1–8, doi:10.2136/vzj2014.07.0089, 2014.
- Koehler, B., Corre, M. d., Veldkamp, E., Wullaert, H. and Wright, S. J.: Immediate and long-term nitrogen oxide emissions from tropical forest soils exposed to elevated nitrogen input, *Glob. Chang. Biol.*, 15, 2049–2066, 2009.
- 545 Körner, C.: The use of “altitude” in ecological research, *Trends Ecol. Evol.*, 22, 569–574, doi:10.1016/j.tree.2007.09.006, 2007.
- Kowalenko, C. G., Ivarson, K. C. and Cameron, D. R.: Effect of moisture content, temperature and nitrogen fertilization on



- carbon dioxide evolution from field soils, *Soil Biol. Biochem.*, 10, 417–423, doi:10.1016/0038-0717(78)90068-8, 1978.
- 550 Kutzbach, L., J., S., Sachs, T., Giebels, M., H., N., Shurpali, N. J., Martikainen, P. J., Alm, J. and Wilmking, M.: CO<sub>2</sub> flux determination by closed-chamber methods can be seriously biased by inappropriate application of linear regression, *Biogeosciences*, 4, 1005–1025, 2007.
- Laughlin, D. C. and Abella, S. R.: Abiotic and biotic factors explain independent gradients of plant community composition in ponderosa pine forests, *Ecol. Modell.*, 205(1–2), 231–240, doi:10.1016/j.ecolmodel.2007.02.018, 2007.
- Leuschner, C., Moser, G., Bertsch, C., Röderstein, M. and Hertel, D.: Large altitudinal increase in tree root/shoot ratio in tropical mountain forests of Ecuador, *Basic Appl. Ecol.*, 8(3), 219–230, doi:10.1016/j.baae.2006.02.004, 2007.
- 555 Luo, Y. and Zhou, X.: Controlling Factors, in *Soil Respiration and the Environment*, pp. 79–105, Elsevier Inc., San Diego, U.S.A., 2006a.
- Luo, Y. and Zhou, X.: Processes of CO<sub>2</sub> production in soil, in *Soil Respiration and the Environment*, pp. 35–59, Elsevier Inc., San Diego, U.S.A., 2006b.
- 560 Luo, Y. and Zhou, X.: Responses to disturbances, in *Soil Respiration and the Environment*, pp. 133–158, Elsevier Inc., San Diego, U.S.A., 2006c.
- Luo, Y. and Zhou, X.: Temporal and spatial variation in soil respiration, in *Soil Respiration and the Environment*, pp. 108–131, Elsevier Inc., San Diego, U.S.A., 2006d.
- Menyailo, O. V. and Hungate, B. A.: Stable isotope discrimination during soil denitrification: Production and consumption of nitrous oxide, *Global Biogeochem. Cycles*, 20, 1–10, doi:10.1029/2005GB002527, 2006.
- Ministerio del Ambiente: Estadísticas de Patrimonio Natural. Datos de bosques, ecosistemas, especies, carbono y deforestación del Ecuador continental [Statistics of Natural Heritage. Data on forests, ecosystems, species, carbon and deforestation of continental Ecuador], Ministerio del Ambiente, Quito, Ecuador., 2015.
- Montzka, S. A., Dlugokencky, E. J. and Butler, J. H.: Non-CO<sub>2</sub> greenhouse gases and climate change, *Nature*, 476, 43–50, doi:10.1038/nature10322, 2011.
- 570 Müller, A. K., Matson, A. L., Corre, M. D. and Veldkamp, E.: Soil N<sub>2</sub>O fluxes along an elevation gradient of tropical montane forests under experimental nitrogen and phosphorus addition, *Front. Earth Sci.*, 3, 1–12, doi:10.3389/feart.2015.00066, 2015.
- Myers, N., Mittermeier, R. A., Mittermeier, C. G., da Fonseca, G. A. B. and Kent, J.: Biodiversity hotspots for conservation priorities, *Nature*, 043, 853–858, doi:10.1080/21564574.1998.9650003, 2000.
- 575 Myhre, G., Shindell, D., Bréon, F.-M., Collins, W., Fuglestedt, J., Huang, J., Koch, D., Lamarque, J.-F., Lee, D., Mendoza, B., Nakajima, T., Robock, A., Stephens, G., Takemura, T. and Zhang, H.: Anthropogenic and natural radiative forcing. *Climate Change 2013: The Physical Science Basis. Contribution of Working Group I to the Fifth Assessment Report of the Intergovernmental Panel on Climate Change*, Cambridge University Press, Cambridge, United Kingdom and New York, NY, USA., 2013.
- 580 Oertel, C., Matschullat, J., Zurba, K., Zimmermann, F. and Erasmi, S.: Greenhouse Gas Emissions From Soil - A review, *Chemie der Erde*, 76, 327–352, doi:10.1016/j.chemer.2016.04.002, 2016.



- Palm, C. A., Alegre, J. C., Arevalo, L., Mutuo, P. K., Mosier, A. R. and Coe, R.: Nitrous oxide and methane fluxes in six different land use systems in the Peruvian Amazon, *Global Biogeochem. Cycles*, 16, 21-1-21–13, doi:10.1029/2001gb001855, 2002.
- 585 Pan, Y., Birdsey, R. A., Fang, J., Houghton, R., Kauppi, P. E., Kurz, W. A., Phillips, O. L., Shvidenko, A., Lewis, S. L., Canadell, J. G., Ciais, P., Jackson, R. B., Pacala, S. W., McGuire, D. A., Piao, S., Rautiainen, A., Sitch, S. and Hayes, D.: A large and persistent carbon sink in the world's forests, *Science* (80-. ), 333, 988–992, 2011.
- Park, S., Pérez, T., Boering, K. A., Trumbore, S. E., Gil, J., Marquina, S. and Tyler, S. C.: Can N<sub>2</sub>O stable isotopes and isotopomers be useful tools to characterize sources and microbial pathways of N<sub>2</sub>O production and consumption in tropical  
590 soils ?, , 25, 1–16, doi:10.1029/2009GB003615, 2011.
- Pérez, T., Trumbore, S. E., Tyler, S. C., Davidson, E. A., Keller, M. and de Carmargo, P. B.: Isotopic variability of N<sub>2</sub>O emissions from tropical forest soils, *Global Biogeochem. Cycles*, 14, 525–535, 2000.
- Persson, T. and Wiren, A.: Microbial activity in forest soils in relation to acid/base and carbon/nitrogen status, in *Air Pollution as Stress Factor in Nordic Forests*, pp. 83–95, Norwegian Institute for Forest Research, Aas., 1989.
- 595 Portmann, R. W., Daniel, J. S. and Ravishankara, A. R.: Stratospheric ozone depletion due to nitrous oxide: influences of other gases, *Phil Trans R Soc B*, 367, 1256–1264, doi:10.1098/rstb.2011.0377, 2012.
- Purbopuspito, J., Veldkamp, E., Brumme, R. and Murdiyarso, D.: Trace gas fluxes and nitrogen cycling along an elevation sequence of tropical montane forests in Central Sulawesi, Indonesia, *Global Biogeochem. Cycles*, 20, 11, doi:10.1029/2005GB002516, 2006.
- 600 Reth, S., Reichstein, M. and Falge, E.: The effect of soil water content, soil temperature, soil pH-value and the root mass on soil CO<sub>2</sub> efflux - a modified model, *Plant Soil*, 268, 21–33, doi:10.1007/s11104-005-0175-5, 2005.
- Silver, W. L., Thompson, A. W., McGroddy, M. E., Varner, R. K., Dias, J. D., Silva, H., Crill, P. M. and Keller, M.: Fine root dynamics and trace gas fluxes in two lowland tropical forest soils, *Glob. Chang. Biol.*, 11, 290–306, doi:10.1111/j.1365-2486.2005.00903.x, 2005.
- 605 Sitaula, B. K., Bakken, L. R. and Abrahamsen, G.: N-fertilization and soil acidification effects on N<sub>2</sub>O and CO<sub>2</sub> emission from temperate pine forest soil, *Soil Biol. Biochem.*, 27, 1401–1408, doi:10.1016/0038-0717(95)00078-S, 1995.
- Sousa Neto, E., Carmo, J. B., Keller, M., Martins, S. C., Alves, L. F., Vieira, S. A., Piccolo, M. C., Camargo, P., Couto, H. T. Z., Joly, C. A. and Martinelli, L. A.: Soil-atmosphere exchange of nitrous oxide, methane and carbon dioxide in a gradient of elevation in the coastal Brazilian Atlantic forest, *Biogeosciences*, 8, 733–742, doi:10.5194/bg-8-733-2011, 2011.
- 610 Su, Q., Domingo-Félez, C., Jensen, M. M. and Smets, B. F.: Abiotic nitrous oxide (N<sub>2</sub>O) production is strongly pH dependent, but contributes little to overall N<sub>2</sub>O emissions in biological nitrogen removal systems, *Environ. Sci. Technol.*, 53, 3508–3516, doi:10.1021/acs.est.8b06193, 2019.
- Syakila, A. and Kroeze, C.: The global nitrous oxide budget revisited, *Greenh. Gas Meas. Manag.*, 1(1), 17–26, doi:10.3763/ghgmm.2010.0007, 2011.
- 615 Teh, Y. A., Diem, T., Jones, S., Huaraca Quispe, L. P., Baggs, E., Morley, N., Richards, M., Smith, P. and Meir, P.: Methane



- and nitrous oxide fluxes across an elevation gradient in the tropical Peruvian Andes, *Biogeosciences*, 11, 2325–2339, doi:10.5194/bg-11-2325-2014, 2014.
- The R Core Team: The R Project for Statistical Computing, [online] Available from: <https://www.r-project.org/> (Accessed 5 March 2019), 2019.
- 620 USDA: Natural Resources Conservation Service. Soil Texture Calculator, [online] Available from: [https://www.nrcs.usda.gov/wps/portal/nrcs/detail/soils/survey/?cid=nrcs142p2\\_054167](https://www.nrcs.usda.gov/wps/portal/nrcs/detail/soils/survey/?cid=nrcs142p2_054167) (Accessed 16 April 2019), 2017.
- Varela, L. A. and Ron, S. R.: Geografía y Clima del Ecuador [Geography and climate of Ecuador]. BIOWEB. Pontificia Universidad Católica del Ecuador., [online] Available from: <https://bioweb.bio/faunaweb/reptiliaweb/GeografiaClima/> (Accessed 2 March 2019), 2018.
- 625 Verchot, L. V., Davidson, E. A., Cattânio, J. H. and Ackerman, I. L.: Land-use change and biogeochemical controls of methane fluxes in soils of eastern Amazonia, *Ecosystems*, 3, 41–56, doi:10.1007/s100210000009, 2000.
- Verhoeven, E., Barthel, M., Yu, L., Celi, L., Said-Pullicino, D., Sleutel, S., Lewicka-Szczebak, D., Six, J. and Decock, C.: Early season N<sub>2</sub>O emissions under variable water management in rice systems: Source-partitioning emissions using isotope ratios along a depth profile, *Biogeosciences*, 16(2), 383–408, doi:10.5194/bg-16-383-2019, 2019.
- 630 Wang, L., Han, Z. and Zhang, X.: Effects of soil pH on CO<sub>2</sub> emission from long-term fertilized black soils in northeastern China, *Sci. Res.*, 58–61, 2010.
- Werner, C., Kiese, R. and Butterbach-Bahl, K.: Soil-atmosphere exchange of N<sub>2</sub>O, CH<sub>4</sub>, and CO<sub>2</sub> and controlling environmental factors for tropical rain forest sites in western Kenya, *J. Geophys. Res.*, 112(D3), D03308, doi:10.1029/2006JD007388, 2007.
- 635 WMO: The State of Greenhouse Gases in the Atmosphere Based on Global Observations through 2018, in *WMO Greenhouse Gas Bulletin.*, vol. 15, pp. 1–8., 2019.
- Wolf, K., Flessa, H. and Veldkamp, E.: Atmospheric methane uptake by tropical montane forest soils and the contribution of organic layers, *Biogeochemistry*, 111, 469–483, doi:10.1007/s10533-011-9681-0, 2012.
- Wrage, N., Velthof, G. L., van Beusichem, M. L. and Oenema, O.: Role of nitrifier denitrification in the production of nitrous  
640 oxide, *Soil Biol. Biochem.*, 33, 1723–1732, 2001.



645 **Table 1.** Characteristics of the study areas Río Silanche (400 m a.s.l.; S\_400), Milpe (1100 m a.s.l.; M\_1100), El Cedral (2200 m a.s.l.; C\_2200) and Peribuela (3010 m a.s.l.; P\_3010), including mean annual precipitations (MAP) and mean annual temperatures (MAT) extracted from the Worldclim data set, using average monthly data from 1970-2000 with a spatial resolution of ~1 km<sup>2</sup> (Fick and R.J. Hijmans, 2017).

Study area	Forest type	Coordinates		Altitude (m a.s.l.)	MAP (mm)	MAT (°C)
		Latitude	Longitude			
<b>S_400</b>	Lowland evergreen forest of Choco	00°08'45.58'' N	79°08'34.22'' W	400	3633	23.0
<b>M_1100</b>	Andean foothill evergreen	00°02'07.17'' N	78°51'59.72'' W	1100	2856	21.1
<b>C_2200</b>	Andean montane evergreen	00°06'47.87'' N	78°34'10.88'' W	2200	1464	16.8
<b>P_3010</b>	Upper montane evergreen	00°22'27.35'' N	78°18'0.36'' W	3010	956	12.8

Note: the coordinates were taken at the center of the plots.



**Table 2.** Physicochemical soil properties of the study areas Río Silanche (400 m a.s.l.; S\_400), Milpe (1100 m a.s.l.; M\_1100), El Cedral (2200 m a.s.l.; C\_2200) and Peribuela (3010 m a.s.l.; P\_3010) at 5 and 20 cm depth, including mean values±standard deviation (SD) of bulk density ( $\rho_b$ ), porosity, pH in water ( $\text{pH}_{\text{water}}$ ) and KCl suspension ( $\text{pH}_{\text{KCl}}$ ),  $\text{NO}_3^-$  and  $\text{NH}_4^+$  concentration, bulk nitrogen (N) and carbon (C) content, carbon-to-nitrogen ratio (C/N) and  $\delta^{15}\text{N}$  signatures from samples of soil taken in August. Similar lowercase letters in superscript and next to some values within one row and per depth (5 and 20 cm) indicate no significant difference at  $P < 0.05$  between sites (S\_400, M\_1100, C\_2200 and P\_3010).

	S_400		M_1100		C_2200		P_3010	
	5 cm	20 cm	5 cm	20 cm	5 cm	20 cm	5 cm	20 cm
<b>Soil class</b>	Andosol <sup>1</sup>		Andosol <sup>1</sup>		Andosol <sup>1</sup>		Andosol <sup>1</sup>	
<b>Soil texture</b>	Loam	Loam	Sandy loam	Sandy loam	Sandy loam	Sandy loam	Loam	Loam
<b>Sand (%)</b>	41.0	40.0	70.8	67.0	63.7	60.5	41.9	45.0
<b>Silt(%)</b>	43.4	47.0	21.7	27.9	29.7	34.4	32.5	34.9
<b>Clay (%)</b>	15.6	13.1	7.6	5.0	6.6	5.2	25.6	20.1
<b><math>\rho_b</math> (g cm<sup>-3</sup>)</b>	0.43±0.15 <sup>b</sup>	0.58±0.07 <sup>b</sup>	0.62±0.09 <sup>a,b</sup>	0.86±0.12 <sup>a</sup>	0.70±0.11 <sup>a</sup>	0.92±0.05 <sup>a</sup>	0.62±0.09 <sup>a,b</sup>	0.81±0.06 <sup>a</sup>
<b>Porosity (%)</b>	83.8±5.5 <sup>a</sup>	78.0±2.5 <sup>a</sup>	76.5±3.3 <sup>a,b</sup>	67.7±4.7 <sup>b</sup>	73.7±4.1 <sup>b</sup>	65.4±2.0 <sup>b</sup>	76.7±3.4 <sup>a,b</sup>	69.6±2.1 <sup>b</sup>
<b><math>\text{pH}_{\text{water}}</math></b>	4.6±0.7 <sup>a,b</sup>	5.2±0.5	4.6±0.8 <sup>b</sup>	5.5±0.4	4.8±0.4 <sup>a,b</sup>	4.8±0.6	5.7±0.5 <sup>a</sup>	5.6±0.5
<b><math>\text{pH}_{\text{KCl}}</math></b>	4.4±0.2 <sup>b</sup>	4.9±0.3 <sup>a,b</sup>	4.5±0.2 <sup>b</sup>	5.0±0.0 <sup>a</sup>	4.5±0.1 <sup>b</sup>	4.6±0.0 <sup>b</sup>	5.1±0.2 <sup>a</sup>	4.9±0.2 <sup>a,b</sup>
<b><math>\text{NO}_3\text{-N}</math> (<math>\mu\text{g g}^{-1}</math>)<sup>2</sup></b>	71.9±39.5 <sup>a</sup>	35.7±29.5 <sup>a</sup>	23.1±15.9 <sup>b</sup>	6.7±7.7 <sup>a,b</sup>	30.6±19.4 <sup>a,b</sup>	7.3±4.3 <sup>a,b</sup>	0.8±0.3 <sup>b</sup>	3.6±7.1 <sup>b</sup>
<b><math>\text{NH}_4\text{-N}</math> (<math>\mu\text{g g}^{-1}</math>)<sup>2</sup></b>	34.3±14.8	27.9±16.1 <sup>a,b</sup>	22.6±4.0	11.9±2.4 <sup>b</sup>	26.5±16.0	18.8±4.9 <sup>b</sup>	22.9±11.3	40.4±13.5 <sup>a</sup>
<b>N (%)</b>	0.8±0.2	0.5±0.1 <sup>a</sup>	0.6±0.2	0.2±0.1 <sup>b</sup>	0.6±0.2	0.3±0.0 <sup>a,b</sup>	0.6±0.0	0.4±0.2 <sup>a,b</sup>
<b>C (%)</b>	8.9±2.4	4.0±1.0 <sup>a,b</sup>	7.1±1.8	2.4±0.7 <sup>b</sup>	6.6±1.7	3.3±0.4 <sup>a,b</sup>	8.6±0.5	4.8±1.5 <sup>a</sup>
<b>C/N<sup>3</sup></b>	10.6±0.4 <sup>c</sup>	8.9±0.4 <sup>c</sup>	11.9±0.6 <sup>b</sup>	10.6±0.7 <sup>b</sup>	11.8±0.8 <sup>b</sup>	10.4±0.5 <sup>b</sup>	14.6±0.5 <sup>a</sup>	12.8±1.3 <sup>a</sup>
<b><math>\delta^{15}\text{N}</math> (‰)<sup>4</sup></b>	6.2±0.5 <sup>a</sup>	8.6±0.9 <sup>a</sup>	6.0±0.8 <sup>a</sup>	6.7±0.8 <sup>b</sup>	4.0±1.2 <sup>b</sup>	4.8±0.5 <sup>c</sup>	3.7±0.6 <sup>b</sup>	4.2±0.4 <sup>c</sup>

Notes: mean values±SD were calculated from soil samples taken adjacent to each soil chamber (n = 5), except for soil texture, where composites for each site at 5 and 20 cm depth were made from the soil samples taken from each chamber. <sup>1</sup>Commonly known as *Andisol* in the USDA Soil Taxonomy; <sup>2</sup>expressed per gram of dry soil; <sup>3</sup>calculated by dividing C (%) by N (%) in each soil sample; and <sup>4</sup>expressed relative to the international standard AIR.



**Table 3.** Average measurements±standard deviations (SD) of CO<sub>2</sub>, CH<sub>4</sub> and N<sub>2</sub>O fluxes at Río Silanche (400 m a.s.l.; S\_400), Milpe (1100 m a.s.l.; M\_1100), El Cedral (2200 m a.s.l.; C\_2200) and Peribuela (3010 m a.s.l.; P\_3010) per month.

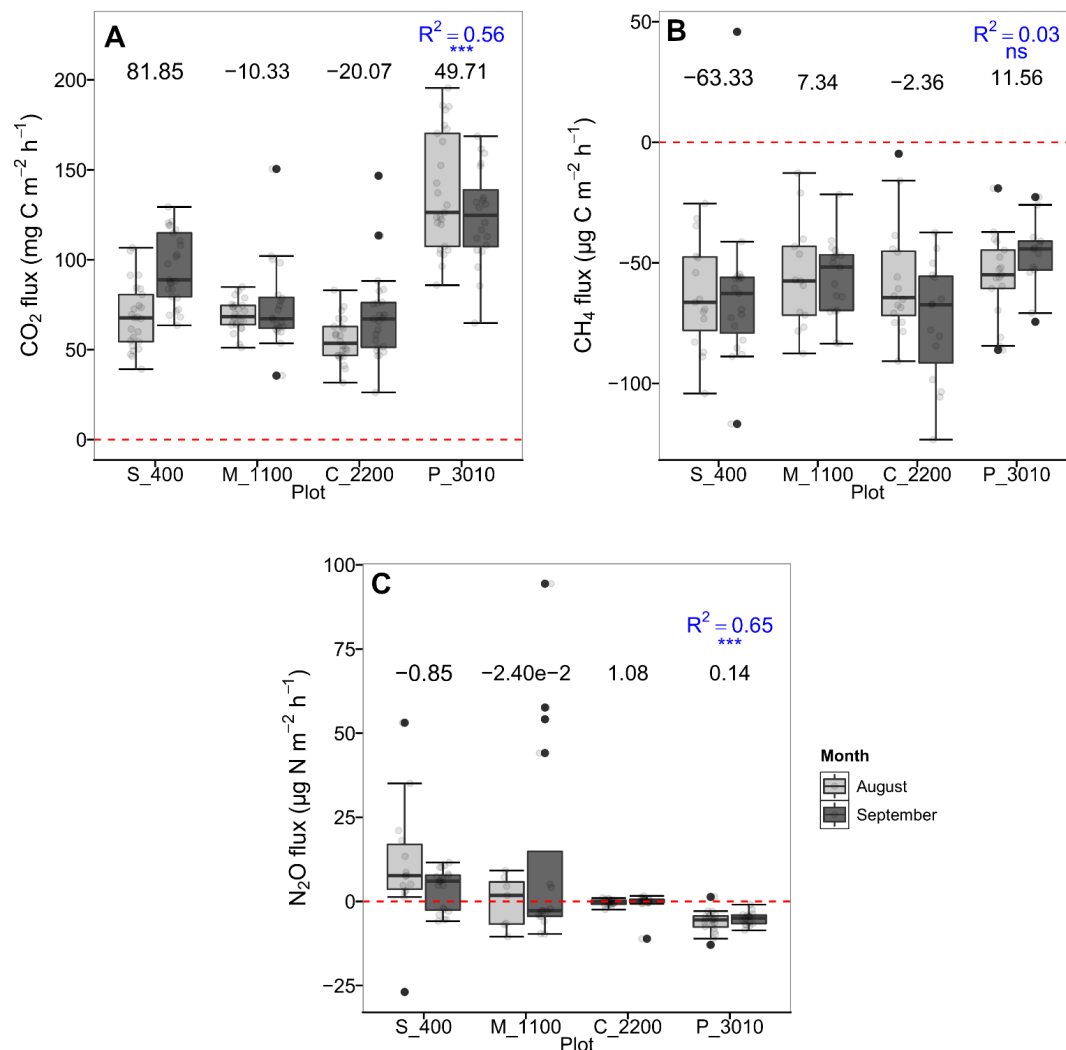
Month	Plot	Average CO <sub>2</sub> flux (mg C m <sup>-2</sup> h <sup>-1</sup> )	Average CH <sub>4</sub> flux (µg C m <sup>-2</sup> h <sup>-1</sup> )	Average N <sub>2</sub> O flux (µg N m <sup>-2</sup> h <sup>-1</sup> )
<b>August</b>	S_400	68.4±18.2	-63.2±22.9	11.1±18.1
	M_1100	69.0±8.5	-55.6±22.3	-0.2±7.7
	C_2200	55.3±12.1	-57.5±22.9	-0.3±0.9
	P_3010	137.6±32.8	-55.5±17.6	-6.1±3.2
<b>September</b>	S_400	95.3±19.9	-63.4±31.7	3.7±6.1
	M_1100	74.6±24.0	-56.3±16.2	13.2±31.3
	C_2200	68.6±24.8	-74.4±25.0	-0.3±2.8
	P_3010	124.0±26.9	-46.7±14.7	-5.1±1.9

Note: flux values represent the mean of 5 chambers per site and per measurement week using the four-point time series and considering the constraint set to evaluate linearity in each measurement cycle ( $R^2 > 0.60$ ).



**Table 4.** Retained predictors of multiple linear regressions for each flux gas (CO<sub>2</sub>, CH<sub>4</sub> and N<sub>2</sub>O) in August.  $\rho_b$  stands for bulk density and “\_5” for properties measured at 5 cm depth. R<sup>2</sup> is the adjusted coefficient of determination, and *P* the significance level of the model. In each case, the R<sup>2</sup> and *P* values reflect the result of the multiple regressions done for each flux and considering all the retained predictors i.e. considering the predictors that are even not significant. ‘ns’, ‘\*’, ‘\*\*’, and ‘\*\*\*’ represent the significant levels of each estimate at *P* > 0.05 (non-significant), 0.01 < *P* ≤ 0.05, 0.001 < *P* ≤ 0.01, and *P* ≤ 0.001, respectively.

Flux response	Predictor	Estimate	<i>P</i> value	R <sup>2</sup>
CO <sub>2</sub>	Intercept	-287.25		
	pH <sub>water_5</sub> ***	73.97	3.21e-07	0.83
	NO <sub>3</sub> <sup>-</sup> -N <sub>5</sub> <sup>ns</sup>	0.129		
CH <sub>4</sub>	-	-	-	-
N <sub>2</sub> O	Intercept	61.96		
	$\rho_b$ _5 <sup>ns</sup>	-34.57	1.40e-02	0.36
	pH <sub>water_5</sub> <sup>ns</sup>	-8.15		



15

**Fig. 1.** A) CO<sub>2</sub> (mg C m<sup>-2</sup> h<sup>-1</sup>), B) CH<sub>4</sub> (µg C m<sup>-2</sup> h<sup>-1</sup>) and C) N<sub>2</sub>O (µg N m<sup>-2</sup> h<sup>-1</sup>) fluxes per month at Río Silanche (400 m a.s.l.; S\_400), Milpe (1100 m a.s.l.; M\_1100), El Cedral (2200 m a.s.l.; C\_2200) and Peribuela (3010 m a.s.l.; P\_3010). Light gray boxplots indicate the fluxes in August 2018, whereas dark gray boxplots, the fluxes in September 2018. Light gray dots in each boxplot represent the measurements taken each day; and black dots, outliers of the respective site. Numbers above the boxplots of each site and per flux gas correspond to the estimated coefficients obtained from a linear model to determine to which extent the sites can explain the variability of the net fluxes; S\_400 is considered as the intercept; R<sup>2</sup> corresponds to the adjusted coefficient of determination of the respective model, and the symbols below it show the significance level of the overall effect at  $P > 0.05$ : 'ns' (non-significant),  $0.01 < P \leq 0.05$ : '\*',  $0.001 < P \leq 0.01$ : '\*\*\*', and  $P \leq 0.001$ : '\*\*\*\*'. Note: N<sub>2</sub>O fluxes were log<sub>10</sub>-transformed.

25

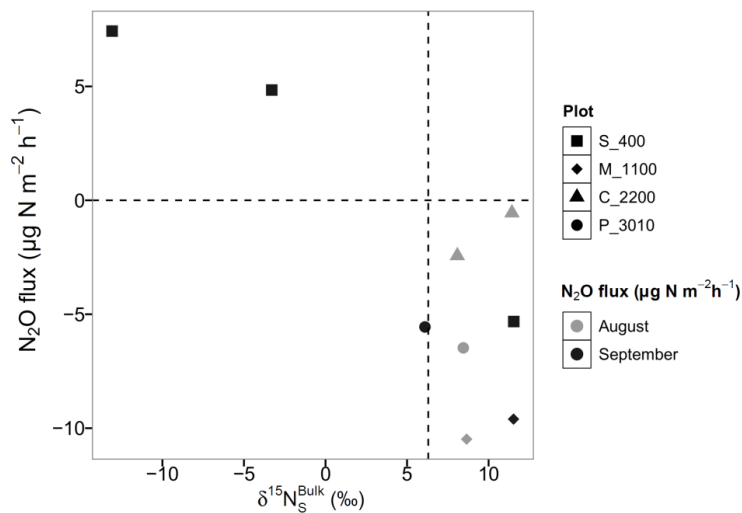
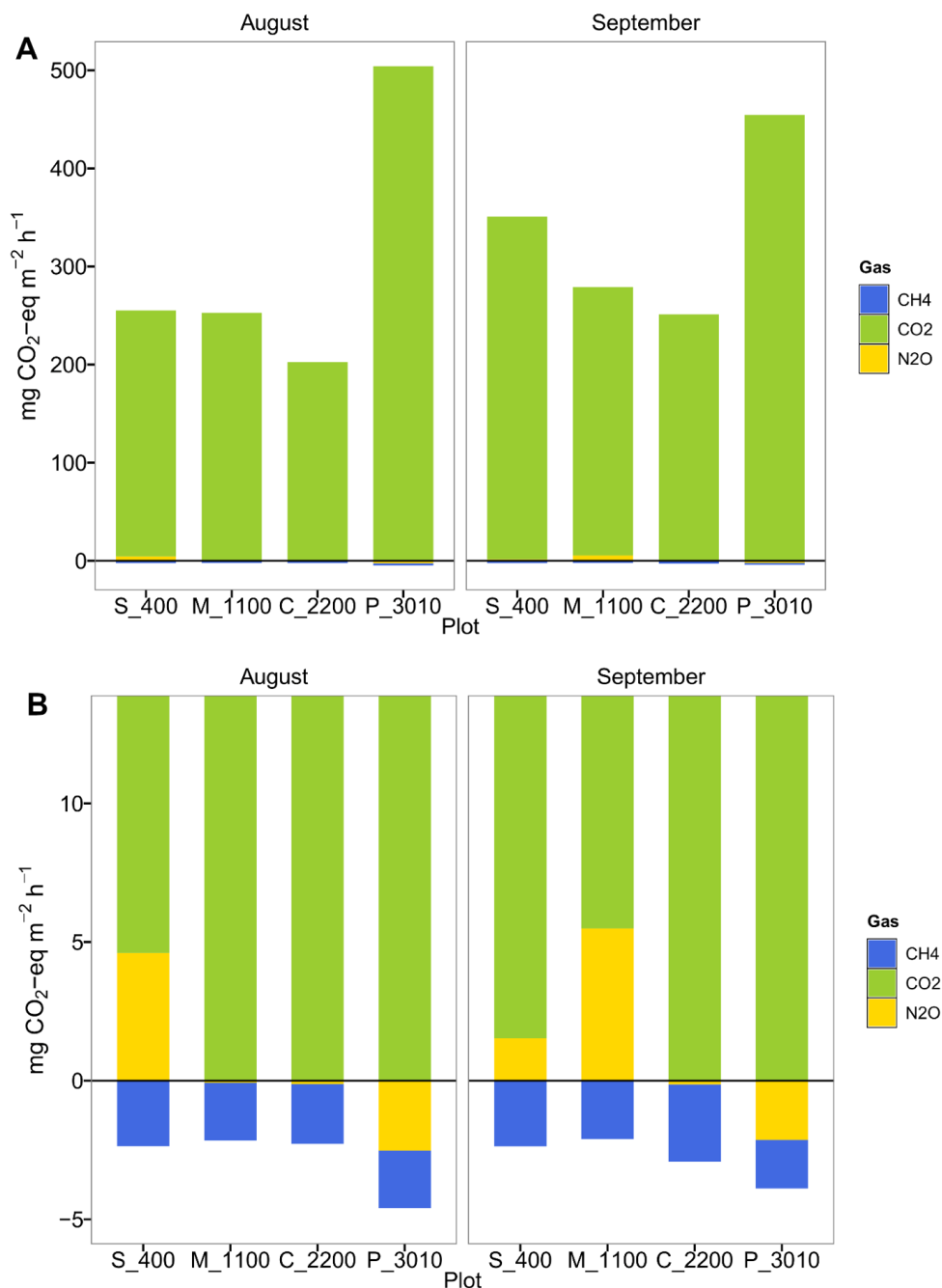


**Fig. 2.** N<sub>2</sub>O fluxes plotted against the bulk isotopic signature of soil N<sub>2</sub>O ( $\delta^{15}N_S^{Bulk}$ ) for point samples taken at Río Silanche - squares (400 m a.s.l.; S\_400), Milpe - diamonds (1100 m a.s.l.; M\_1100), El Cedral - triangles (2200 m a.s.l.; C\_2200) and 30 Peribuela - circles (3010 m a.s.l.; P\_3010) during August (grey) and September (black). Note: the dotted x axis at 6.3‰ represents the atmospheric bulk N<sub>2</sub>O composition (Harris et al., 2017), and  $\delta^{15}N_S^{Bulk}$  values were calculated based on a two-source mixing model, considering a threshold of 20 ppb to exclude low fluxes and thus, avoid larger uncertainties in the source calculation.



35

**Fig. 3.** CO<sub>2</sub> equivalent (CO<sub>2</sub>-eq) emissions at Río Silanche (400 m a.s.l.; S\_400), Milpe (1100 m a.s.l.; M\_1100), El Cedral (2200 m a.s.l.; C\_2200) and Peribuela (3010 m a.s.l.; P\_3010) during August and September 2018, and expressed as mg CO<sub>2</sub>-eq m<sup>-2</sup> h<sup>-1</sup>. Positive values indicate emission of GHGs whereas negative, consumption. Blue bars show the CO<sub>2</sub>-eq emissions (-) of CH<sub>4</sub>, green (+) of CO<sub>2</sub> and yellow (+ and -) of N<sub>2</sub>O, using a global warming potential (GWP) of 1, 28 and 265, in each case and over a 100-year time horizon (Myhre et al., 2013). Figure B) is a zoom-in view of figure A).

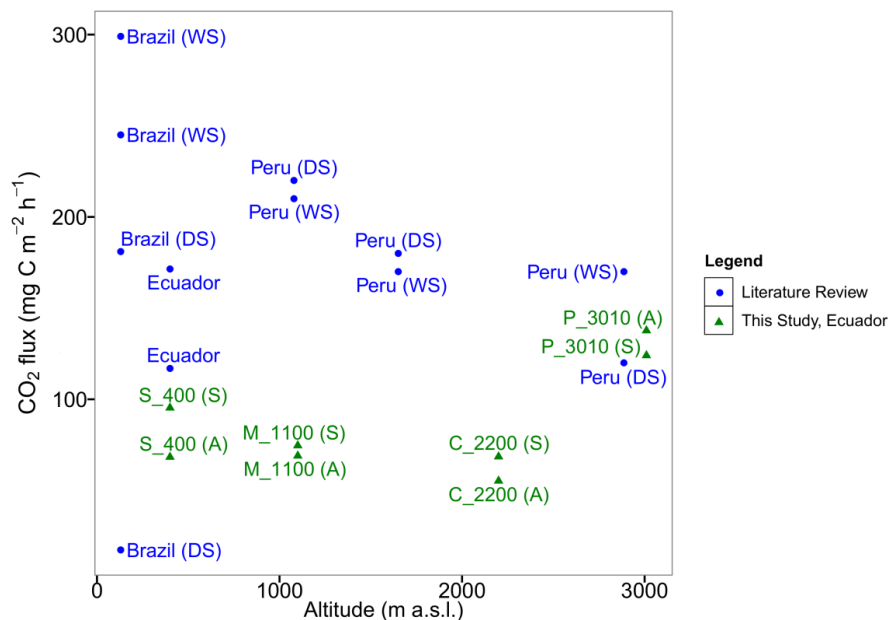


**Fig. 4.** Comparison of CO<sub>2</sub> fluxes with different studies. Blue dots: CO<sub>2</sub> fluxes reported in literature for South America (Table S.3); “DS” stands for fluxes taken specifically during a dry season, whereas “WS” during a wet season. Green triangles: CO<sub>2</sub> fluxes obtained in this study for Río Silanche (400 m a.s.l.; S\_400), Milpe (1100 m a.s.l.; M\_1100), El Cedral (2200 m a.s.l.; C\_2200) and Peribuela (3010 m a.s.l.; P\_3010); ‘(A)’ denotes the fluxes obtained in August - end of the dry season in the region, and ‘(S)’ the fluxes obtained in September – beginning of the rainy season.

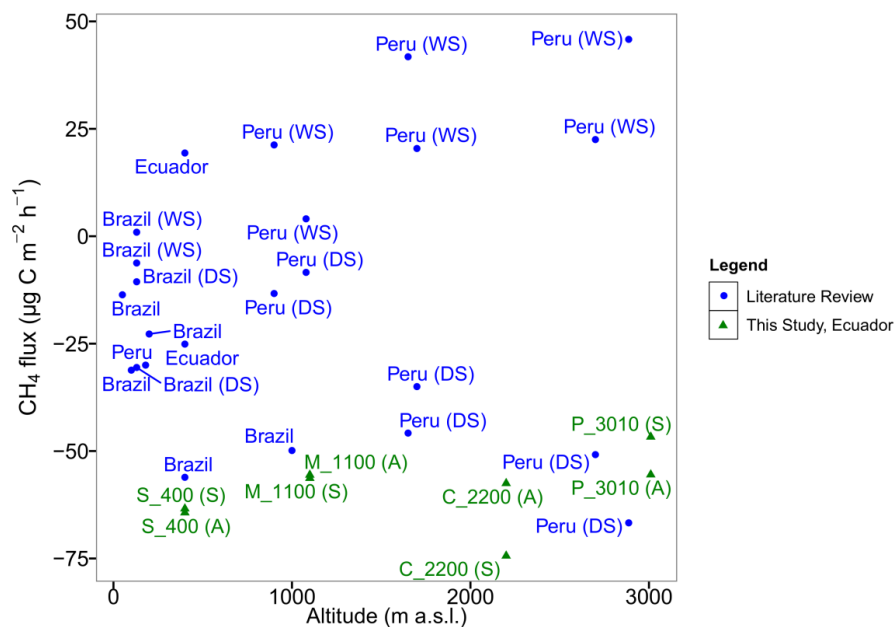


**Fig. 5.** Comparison of CH<sub>4</sub> fluxes with different studies. Blue dots: CH<sub>4</sub> fluxes reported in literature for South America (Table S.3); “DS” stands for fluxes taken specifically during a dry season, whereas “WS” during a wet season. Green triangles: CH<sub>4</sub> fluxes obtained in this study for Río Silanche (400 m a.s.l.; S\_400), Milpe (1100 m a.s.l.; M\_1100), El Cedral (2200 m a.s.l.; C\_2200) and Peribuela (3010 m a.s.l.; P\_3010); ‘(A)’ denotes the fluxes obtained in August - end of the dry season in the region, and ‘(S)’ the fluxes obtained in September – beginning of the rainy season.



55

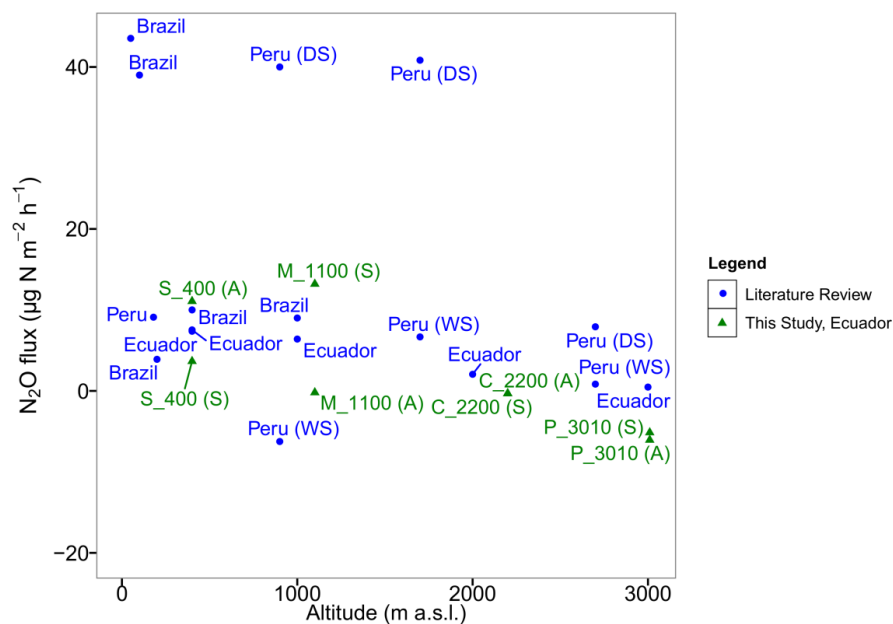


**Fig. 6.** Comparison of N<sub>2</sub>O fluxes with different studies. Blue dots: N<sub>2</sub>O fluxes reported in literature for South America (Table S.3); “DS” stands for fluxes taken specifically during a dry season, whereas “WS” during a wet season. Green triangles: N<sub>2</sub>O fluxes obtained in this study for Río Silanche (400 m a.s.l.; S\_400), Milpe (1100 m a.s.l.; M\_1100), El Cedral (2200 m a.s.l.; C\_2200) and Peribuela (3010 m a.s.l.; P\_3010); ‘(A)’ denotes the fluxes obtained in August - end of the dry season in the region, and ‘(S)’ the fluxes obtained in September – beginning of the rainy season.